

On Stein’s test of uniformity on the hypersphere

Paul Axmann^{1,3}, Bruno Ebner¹, and Eduardo García-Portugués²

Abstract

We propose a new test of uniformity on the hypersphere based on a Stein characterization associated with the Laplace–Beltrami operator. We identify a sufficient class of test functions for this characterization, linked to the moment generating function. Exploiting the operator’s eigenfunctions to obtain a harmonic decomposition in terms of Gegenbauer polynomials, we show that the proposed procedure belongs to the class of Sobolev tests. We derive closed-form expressions for the distribution of the test statistic under the null hypothesis and under fixed alternatives. To enhance power against a range of alternatives, we introduce a tuning parameter into the characterization and study its impact on rejection probabilities. We discuss data-driven strategies for selecting this parameter to maximize rejection rates for a given alternative and compare the resulting performance with that of related parametric tests. Additional numerical experiments compare the proposed test with competing Sobolev-class procedures, highlighting settings in which it offers clear advantages.

Keywords: Directional data; Laplace–Beltrami operator; Sobolev tests; Uniformity; Stein characterization.

1 Introduction

Stein operators offer a powerful tool for characterizing probability distributions and can be naturally applied to construct goodness-of-fit tests. The use of distributional characterizations to design goodness-of-fit procedures dates back to Yu. V. Linnik in the early 1950s (Linnik, 1953a,b; Nikitin, 2017). However, Stein-characterization-based approaches to testing uniformity on hyperspheres have only recently begun to be explored, and their relationship to classical uniformity tests remains underdeveloped. Recent works presenting new uni- and multivariate (Euclidean) procedures exploit Stein characterizations and build L^2 -type test statistics that quantify the magnitude of the expectation of a Stein operator evaluated over a characterizing class of functions; see Anastasiou et al. (2023). We adopt this framework for testing uniformity in directional statistics, where the relevant Stein operator is the Laplace–Beltrami operator, i.e., the spherical component of the Euclidean Laplacian. Directional statistics concerns observations that represent directions; equivalently, it studies random points supported on the unit (hyper)sphere $\mathcal{S}^{p-1} := \{\mathbf{x} \in \mathbb{R}^p : \|\mathbf{x}\| = 1\}$, where the ambient dimension is $p \geq 2$. Fundamental techniques and results are presented in the monographs by Mardia and Jupp (1999) and Ley and Verdebout (2017), and recent developments are reviewed in Pewsey and García-Portugués (2021) and García-Portugués and Verdebout (2018).

When considering directional data, uniformity is among the most fundamental properties to address. Formally, for an independent and identically distributed (iid) sample $\mathbf{X}_1, \dots, \mathbf{X}_n \sim \mathbb{P}$ on the sphere, $n \in \mathbb{N}$, the hypothesis

$$\mathcal{H}_0 : \mathbb{P} = \text{Unif}(\mathcal{S}^{p-1}) \text{ vs. } \mathcal{H}_1 : \mathbb{P} \neq \text{Unif}(\mathcal{S}^{p-1})$$

is tested. This classical problem has been widely studied, with some of the most relevant tests being the Rayleigh (1919) test based on the first moments, the Bingham (1974) test based on second order moments, and the Giné (1975) F_n test, based on an expansion in spherical harmonics. In

¹Institute of Stochastics, Karlsruhe Institute of Technology (Germany).

²Department of Statistics, Carlos III University of Madrid (Spain).

³Corresponding author. e-mail: paul.axmann@kit.edu.

addition, more recent proposals include projection-based classes of tests (García-Portugués et al., 2023; Borodavka and Ebner, 2026) and tests based on the Poisson kernel (Fernández-de-Marcos and García-Portugués, 2023; Ding et al., 2025). Closely related to our setting, Fernández-de-Marcos and García-Portugués (2023) also introduce a softmax test based on the von Mises–Fisher kernel, which involves a tuning parameter. Many of these tests belong to the class of Sobolev tests introduced in Beran (1968) and Giné (1975). Within this common framework, Cutting et al. (2017) and Ebner et al. (2025) derive the asymptotic null distribution as the dimension diverges to infinity, while García-Portugués et al. (2026) establishes detection thresholds for rotationally symmetric alternatives. Another relevant approach is the directional kernel Stein discrepancy (dKSD) test of Xu and Matsuda (2020), employing Stein operators on the sphere or more general extensions to Riemannian manifolds (Barp et al., 2022; Qu and Vemuri, 2025; Xu and Matsuda, 2021).

Our characterization approach relies on Stein’s method (Stein, 1972; Chen et al., 2011), and the proposed testing procedure follows the construction outlined in Anastasiou et al. (2023, Section 5.2). The main idea is to apply a suitable Stein operator \mathcal{A} to a characterizing parametric function class \mathcal{F} , so that $\mathbb{E}[\mathcal{A}f(\mathbf{X})] = 0$ holds for all $f \in \mathcal{F}$, if and only if the distribution of \mathbf{X} satisfies the hypothesis \mathcal{H}_0 . This characterization naturally leads to a test statistic by replacing the expectation with its empirical counterpart. As the empirical mean consistently estimates the expectation, the statistic converges to zero under \mathcal{H}_0 , while “large” deviations from zero imply rejection of \mathcal{H}_0 in favor of \mathcal{H}_1 . In our setting, with a uniform target distribution, a characterization induced by the Laplace–Beltrami operator is practically useful: for all smooth functions f , we have $\mathbb{E}[\Delta_{\mathcal{S}^{p-1}}f(\mathbf{X})] = 0$ exactly for uniformly distributed random unit vectors \mathbf{X} .

This is a special case of the second-order Stein operator \mathcal{A} in Fischer et al. (2026) and Barp et al. (2022) for general target distributions on \mathcal{S}^{p-1} with density q , which can also be found for local coordinates in Xu and Matsuda (2021). There, the spherical Stein operator

$$\mathcal{A}f := \Delta_{\mathcal{S}^{p-1}}f + \langle \nabla \log(q), \nabla_{\mathcal{S}^{p-1}}f \rangle_{\mathbb{R}^p}, \quad (1)$$

is derived through Green’s first identity. In the uniform case, the density q is constant, implying $\langle \nabla \log(q), \nabla_{\mathcal{S}^{p-1}}f \rangle_{\mathbb{R}^p} = 0$ for all f , so the Stein operator simplifies to the Laplace–Beltrami operator $\Delta_{\mathcal{S}^{p-1}}$. Note that, up to a multiplicative constant, this Stein operator coincides with the infinitesimal generator of spherical Brownian motion (Hsu, 2002, Chapter 3), whose stationary distribution is the uniform law on the sphere; it is therefore directly connected to the so-called generator approach to find Stein operators (Barbour, 1988, 1990).

To construct the test statistic, we further need a parametric class of test functions that is rich enough to characterize the distribution through the Stein identity induced by the operator. Here, we choose the class $\{e^{\lambda \mathbf{t}^\top \mathbf{x}} : \mathbf{t} \in \mathcal{S}^{p-1}\}$, $\lambda > 0$ fixed, connecting the test to the moment generating function (mgf) $M_{\mathbf{X}}(\mathbf{t}) = \mathbb{E}[e^{\mathbf{t}^\top \mathbf{X}}]$, $\mathbf{t} \in \mathbb{R}^p$. Plugging in this class of test functions leads to the following characterization of the uniform law that we prove in Appendix A.

Proposition 1.1. *Let $p \geq 2$ and $\lambda > 0$. Let \mathbf{X} be an absolutely continuous random vector on \mathcal{S}^{p-1} . Then, we have the characterization*

$$\begin{cases} \mathbb{E}[\Delta_{\mathcal{S}^{p-1}}e^{\lambda \mathbf{t}^\top \mathbf{X}}] = \Delta_{\mathcal{S}^{p-1}}M_{\mathbf{X}}(\lambda \mathbf{t}) = 0, \mathbf{t} \in \mathcal{S}^{p-1} \\ M_{\mathbf{X}}(\mathbf{0}) = 1, \end{cases} \quad \text{if and only if } \mathbf{X} \sim \text{Unif}(\mathcal{S}^{p-1}). \quad (2)$$

To build a test statistic using this characterization of the uniform distribution, we evaluate the expectation $\mathbb{E}[\Delta_{\mathcal{S}^{p-1}}e^{\lambda \mathbf{t}^\top \mathbf{X}}]$ for all $\mathbf{t} \in \mathcal{S}^{p-1}$. To this end, we consider the square-integrable map $\mathbf{t} \mapsto \mathbb{E}[\Delta_{\mathcal{S}^{p-1}}e^{\lambda \mathbf{t}^\top \mathbf{X}}]$. More precisely, let ν_{p-1} denote the uniform probability measure on \mathcal{S}^{p-1} , so $\nu_{p-1}(\mathcal{S}^{p-1}) = 1$, and consider the Hilbert space $L^2(\mathcal{S}^{p-1})$ of square-integrable functions on the sphere with scalar product $\langle h, k \rangle_{L^2(\mathcal{S}^{p-1})} = \int_{\mathcal{S}^{p-1}} h(\mathbf{x})k(\mathbf{x}) d\nu_{p-1}(\mathbf{x})$ for all $h, k \in L^2(\mathcal{S}^{p-1})$ with the corresponding norms. Then, we define the population discrepancy

$$T(\lambda) := \left\| \mathbb{E}[\Delta_{\mathcal{S}^{p-1}}e^{\lambda \mathbf{t}^\top \mathbf{X}}] \right\|_{L^2(\mathcal{S}^{p-1})}^2$$

to characterize the distribution of \mathbf{X} . Since rotational invariance with respect to all rotations about the origin is a well-known characterizing property of the uniform distribution on the sphere, we construct a rotation-invariant test by uniformly integrating over directions using the unweighted L^2 norm. Now, given $n \in \mathbb{N}$ iid copies $\mathbf{X}_1, \dots, \mathbf{X}_n$ of the random element \mathbf{X} on S^{p-1} , we approximate the expectation $\mathbb{E}[\Delta_{S^{p-1}} e^{\lambda t^\top \mathbf{X}}]$ by the empirical mean to propose the test statistic

$$\begin{aligned} T_n(\lambda) &:= n \left\| \frac{1}{n} \sum_{j=1}^n \Delta_{S^{p-1}} e^{\lambda t^\top \mathbf{X}_j} \right\|_{L^2(S^{p-1})}^2 \\ &= \frac{1}{n} \sum_{i,j=1}^n \int_{S^{p-1}} \Delta_{S^{p-1}} e^{\lambda t^\top \mathbf{X}_i} \Delta_{S^{p-1}} e^{\lambda t^\top \mathbf{X}_j} d\nu_{p-1}(\mathbf{t}). \end{aligned} \quad (3)$$

This statistic can be computed efficiently, through the forthcoming decomposition (8).

The remainder of the paper is organized as follows. Starting from our Stein-type construction, we derive a closed-form representation of the proposed test statistic. Our main tool is a Gegenbauer (spherical harmonic) decomposition of the test functions. Exploiting orthogonality and their connection to the Laplace–Beltrami operator, we lift the decomposition from the test-function level to a decomposition of the entire statistic, yielding an explicit series expansion. This representation is computationally convenient, allows us to establish the characterization (2) and to develop an asymptotic theory both at the level of the underlying process and for the evaluated statistic. We treat the null case \mathcal{H}_0 as well as fixed alternatives, and provide simplified expressions for rotationally symmetric alternatives. We further analyze the effect of tuning, including boundary/limit regimes. The harmonic viewpoint places the procedure within the class of Sobolev tests. We derive a direct link between our Stein test and arbitrary Sobolev tests. In addition, we compare our method to a kernel Stein discrepancy (dKSD) test, derive an analogous harmonic decomposition for dKSD, and thus obtain the explicit asymptotic results from this test statistic. In simulations, we provide plots to illustrate how the tuning parameter shapes the covariance kernel and the limiting random field predicted by the asymptotic theory. Based on the results from the asymptotic section, we describe a tuning approach for the concentration parameter to optimize power against a given alternative by maximizing the standardized mean shift. Across a range of alternative distributions, we demonstrate its substantial impact on power and empirically validate the proposed tuning strategy. Here, we further observe the empirical power of the test compared to other uniformity tests. We close the paper with a discussion. Proofs are relegated to the appendix.

2 Spherical harmonic decomposition of the test statistic

To obtain an explicit decomposition of the test statistic, we reduce integrals of zonal functions to one-dimensional integrals. For $p \geq 2$, define

$$L^{2,p} := L^2([-1, 1], (1 - u^2)^{(p-3)/2} du), \quad \langle f, g \rangle_{L^{2,p}} := \int_{-1}^1 f(u)g(u)(1 - u^2)^{(p-3)/2} du,$$

for $f, g \in L^{2,p}$. In dimension $p \geq 3$, the Gegenbauer polynomials $\{C_k^{(p-2)/2}\}_{k=0}^\infty$ form an orthogonal basis of $L^{2,p}$, where k denotes the degree of the polynomial, while in the case $p = 2$, the Chebyshev polynomials $C_k^0(u) := \cos(k \arccos(u))$ for all $k \in \mathbb{N}_0$ form an orthogonal basis of $L^{2,2}$. To unify notation, we denote the Chebyshev polynomials by $\{C_k^0\}_{k=0}^\infty$, as they form a limit to the Gegenbauer polynomials, making them a natural choice to extend the Gegenbauer construction to the circular case:

$$\lim_{\nu \rightarrow 0^+} \frac{1}{\nu} C_k^\nu(u) = \frac{2}{k} C_k^0(u), \quad \text{for } k \geq 1.$$

Further, let $\omega_m = 2\pi^{(m+1)/2}/\Gamma((m+1)/2)$ denote the Lebesgue surface measure of the unit sphere \mathcal{S}^m for all $m \in \mathbb{N}$. Then, for $\mathbf{t}, \mathbf{x} \in \mathcal{S}^{p-1}$ and any zonal function $f_{\mathbf{t}}(\mathbf{x}) = f(\mathbf{x}^\top \mathbf{t})$, the change of variables

$$\int_{\mathcal{S}^{p-1}} f(\mathbf{x}^\top \mathbf{t}) d\nu_{p-1}(\mathbf{x}) = \frac{\omega_{p-2}}{\omega_{p-1}} \int_{-1}^1 f(u)(1-u^2)^{(p-3)/2} du$$

connects the spaces $L^2(\mathcal{S}^{p-1})$ and $L^{2,p}$, by reducing integrals of zonal functions on \mathcal{S}^{p-1} to integrals on $[-1, 1]$ with the corresponding weight.

For $\mathbf{t}, \mathbf{x} \in \mathcal{S}^{p-1}$, we consider an orthogonal expansion of the function $f_\lambda(u) := e^{\lambda u}$ in $L^{2,p}$ with $\mathbf{t}^\top \mathbf{x} = u \in [-1, 1]$ and $\lambda > 0$ using Gegenbauer or Chebyshev polynomials, depending on the dimension. With the coefficients defined as

$$m_{k,p}(\lambda) := \frac{\langle f_\lambda, C_k^{(p-2)/2} \rangle_{L^{2,p}}}{\|C_k^{(p-2)/2}\|_{L^{2,p}}^2}, \quad e^{\lambda u} = \sum_{k=0}^{\infty} m_{k,p}(\lambda) C_k^{(p-2)/2}(u), \quad u \in [-1, 1], \quad (4)$$

the orthogonal expansion converges in $L^{2,p}$ and, for fixed \mathbf{t} with $u = \mathbf{t}^\top \mathbf{x}$, as a function in \mathbf{x} in $L^2(\mathcal{S}^{p-1})$, see Dai and Xu (2013, Theorem 2.2.2). For smooth functions such as the exponential, the coefficients decay rapidly, and the series further converges uniformly on $[-1, 1]$, which allows term-wise application of the Laplace–Beltrami operator in the following derivations.

Remark 2.1. *The uniform convergence of $e^{\lambda \mathbf{t}^\top \mathbf{x}} = \sum_{k=0}^{\infty} m_{k,p}(\lambda) C_k^{(p-2)/2}(\mathbf{t}^\top \mathbf{x})$ holds since $\mathbf{x} \mapsto e^{\lambda \mathbf{t}^\top \mathbf{x}}$ is infinitely differentiable on \mathcal{S}^{p-1} (Kalf, 1995, Theorem 2).*

To obtain a closed-form expression of $m_{k,p}(\lambda)$ for $p \geq 3$, we use an integral identity of Bessel functions

$$\frac{1}{h_{k,p}} \int_{-1}^1 e^{au} C_k^{(p-2)/2}(u)(1-u^2)^{(p-3)/2} du = \left(\frac{2}{a}\right)^{(p-2)/2} \Gamma\left(\frac{p-2}{2}\right) \left(k + \frac{p-2}{2}\right) \mathcal{I}_{(p-2)/2+k}(a),$$

which follows from Zwillinger et al. (2014, Formula 7.321) using $h_{k,p} = \|C_k^{(p-2)/2}\|_{L^{2,p}}^2$ and $a \in \mathbb{C} \setminus \{0\}$. Here, \mathcal{I}_k denotes the modified Bessel function of the first kind and order k . The case $p = 2$ is obtained analogously, by applying DLMF (2020, 18.3.1) and DLMF (2020, 10.9.2). As a result, setting $a = \lambda > 0$, it follows that

$$m_{k,p}(\lambda) = \begin{cases} (2 - 1_{\{k=0\}}) \mathcal{I}_k(\lambda), & p = 2, \\ \left(\frac{2}{\lambda}\right)^{(p-2)/2} \Gamma\left(\frac{p-2}{2}\right) \left(k + \frac{p-2}{2}\right) \mathcal{I}_{(p-2)/2+k}(\lambda), & p > 2, \end{cases} \quad (5)$$

a quantity that will appear throughout the paper.

We introduce the constant

$$\gamma_{k,p} := \begin{cases} \frac{1 + 1_{\{k=0\}}}{2}, & p = 2, \\ \frac{p-2}{2k+p-2}, & p > 2, \end{cases} \quad (6)$$

to unify the notation. Using this notation, we use the Funk–Hecke formula (Dai and Xu, 2013, Theorem 1.2.9) to have

$$\int_{\mathcal{S}^{p-1}} C_k^{(p-2)/2}(\mathbf{t}^\top \mathbf{x}) C_k^{(p-2)/2}(\mathbf{y}^\top \mathbf{t}) d\nu_{p-1}(\mathbf{t}) = \gamma_{k,p} C_k^{(p-2)/2}(\mathbf{x}^\top \mathbf{y}). \quad (7)$$

The series expansion (4) is particularly convenient because, for any fixed $\mathbf{t} \in \mathcal{S}^{p-1}$, the Gegenbauer polynomials satisfy $\Delta_{\mathcal{S}^{p-1}} C_k^{(p-2)/2}(\mathbf{t}^\top \mathbf{x}) = (-k)(k+p-2) C_k^{(p-2)/2}(\mathbf{t}^\top \mathbf{x})$; see Property 2 in Dai

and Xu (2013, Section B.2). Hence, the Gegenbauer polynomials $C_k^{(p-2)/2}(\mathbf{t}^\top \mathbf{x})$ are eigenfunctions of the Laplace–Beltrami operator $\Delta_{\mathcal{S}^{p-1}}$ with eigenvalues $(-k)(k+p-2)$.

The case $p = 2$ simplifies further, since the space \mathcal{S}^1 is one-dimensional. With $\mathbf{x} = (\cos \theta, \sin \theta)^\top$, for a function f on \mathcal{S}^1 , the Laplace–Beltrami operator reduces to

$$\Delta_{\mathcal{S}^1} f(\theta) = \frac{d^2}{d\theta^2} f(\theta)$$

see Dai and Xu (2013, Section 1.6.1) and thus the Chebyshev polynomials satisfy $\Delta_{\mathcal{S}^1} C_k^0(\mathbf{t}^\top \mathbf{x}) = -k^2 C_k^0(\mathbf{t}^\top \mathbf{x})$, hence they are eigenfunctions of the Laplace–Beltrami operator on \mathcal{S}^1 corresponding to the eigenvalues $-k^2$.

Using the Expansion (4), its uniform convergence in $[-1, 1]$ and the linearity of $\Delta_{\mathcal{S}^{p-1}}$, we apply the operator $\Delta_{\mathcal{S}^{p-1}}$ to the expansion of $e^{\lambda \mathbf{t}^\top \mathbf{x}}$, hence for $p \geq 2$

$$\begin{aligned} \Delta_{\mathcal{S}^{p-1}} e^{\lambda \mathbf{t}^\top \mathbf{x}} &= \Delta_{\mathcal{S}^{p-1}} \sum_{k=0}^{\infty} m_{k,p}(\lambda) C_k^{(p-2)/2}(\mathbf{t}^\top \mathbf{x}) = \sum_{k=0}^{\infty} m_{k,p}(\lambda) \Delta_{\mathcal{S}^{p-1}} C_k^{(p-2)/2}(\mathbf{t}^\top \mathbf{x}) \\ &= \sum_{k=0}^{\infty} (m_{k,p}(\lambda) (-k)(k+p-2)) C_k^{(p-2)/2}(\mathbf{t}^\top \mathbf{x}) \end{aligned}$$

holds. With these observations, the test statistic takes the following series representation. Its proof, as with all the proofs of the paper, can be found in Appendix A.

Lemma 2.1. *Let $\lambda > 0$. Then $T_n(\lambda)$ has a harmonic decomposition of the form*

$$T_n(\lambda) = \frac{1}{n} \sum_{i,j=1}^n \sum_{k=1}^{\infty} c_{k,p}(\lambda) C_k^{(p-2)/2}(\mathbf{X}_i^\top \mathbf{X}_j), \quad (8)$$

where the coefficients satisfy

$$c_{k,p}(\lambda) := (m_{k,p}(\lambda) k(k+p-2))^2 \gamma_{k,p} \quad \text{for } k \in \mathbb{N}, p \geq 2.$$

The coefficients are

$$c_{k,p}(\lambda) = \begin{cases} 2k^4 \mathcal{I}_k(\lambda)^2, & p = 2, \\ 2^{p-3} \lambda^{2-p} (p-2) \left(k + \frac{p-2}{2}\right) \left(\Gamma\left(\frac{p-2}{2}\right) k(k+p-2) \mathcal{I}_{(p-2)/2+k}(\lambda)\right)^2, & p > 2. \end{cases} \quad (9)$$

Lemma 2.1 delivers a closed-form formula of the test statistic in (3). In practice, it is sufficient to consider the truncated series (8), since the coefficients $c_{k,p}(\lambda)$ decay exponentially in k . Obviously, (3) is a Sobolev test in the sense of Giné (1975), for more details, see Section 4.2. In the further analysis, including fixed alternative distributions, we introduce notation for a general spherical harmonic basis.

Let k denote the degree of the spherical harmonics, then the set $\{Y_{r,k} : r = 1, \dots, d_{k,p}\}$ spans the degree- k space of spherical harmonics, with dimension $d_{k,p} = \binom{p+k-3}{p-2} + \binom{p+k-2}{p-2}$. Then $\{Y_{r,k} : k \in \mathbb{N}_0, r = 1, \dots, d_{k,p}\}$ forms an orthonormal basis of the space of spherical harmonics \mathcal{H}^p with respect to the uniform measure ν_{p-1} . Since the space of spherical harmonics is dense in $L^2(\mathcal{S}^{p-1})$, the spherical harmonics also form a basis of $L^2(\mathcal{S}^{p-1})$ (Dai and Xu, 2013, Theorem 2.2.2.).

Details on this construction can be found in García-Portugués et al. (2026, Section 3). If $q \in L^2(\mathcal{S}^{p-1})$ is a density on \mathcal{S}^{p-1} , then it admits the harmonic expansion

$$q(\mathbf{x}) = \sum_{k=0}^{\infty} \sum_{r=1}^{d_{k,p}} \beta_{r,k} Y_{r,k}(\mathbf{x}) \quad \text{in } L^2(\mathcal{S}^{p-1}), \quad (10)$$

with coefficients

$$\beta_{r,k} = \int_{\mathcal{S}^{p-1}} q(\mathbf{x}) Y_{r,k}(\mathbf{x}) d\nu_{p-1}(\mathbf{x}). \quad (11)$$

Note that here the equality is given in the sense that

$$\lim_{n \rightarrow \infty} \left\| q - \sum_{k=0}^n \sum_{r=1}^{d_{k,p}} \beta_{r,k} Y_{r,k} \right\|_{L^2(\mathcal{S}^{p-1})} = 0.$$

3 Asymptotic results

To analyze the asymptotic behavior of the test statistic, we define the $L^2(\mathcal{S}^{p-1})$ -valued random element $W_n : \mathcal{S}^{p-1} \rightarrow \mathbb{R}$ by

$$W_n(\mathbf{t}) := \frac{1}{\sqrt{n}} \sum_{i=1}^n \sum_{k=1}^{\infty} (m_{k,p}(\lambda) (-k)(k+p-2)) C_k^{(p-2)/2}(\mathbf{t}^\top \mathbf{X}_i), \quad \mathbf{t} \in \mathcal{S}^{p-1},$$

so that $T_n(\lambda) = \|W_n\|_{L^2(\mathcal{S}^{p-1})}^2$. Obviously $\{W_n(\mathbf{t}) : \mathbf{t} \in \mathcal{S}^{p-1}\}$ is a real-valued random field indexed by \mathcal{S}^{p-1} .

3.1 Limits under \mathcal{H}_0

We first derive closed-form expressions of the limiting null distribution. Since $T_n(\lambda)$ can be represented as the norm of a sum of iid L^2 -valued random elements, an application of the central limit theorem in separable Hilbert spaces (Henze, 2024, Theorem 17.29) and the continuous mapping theorem are used to prove the following result.

Theorem 3.1. *Let $p \geq 2$ and let $\mathbf{X}_1, \dots, \mathbf{X}_n$ be iid uniformly distributed random vectors on the sphere \mathcal{S}^{p-1} . Then, as $n \rightarrow \infty$, there exists a centered Gaussian random element \mathcal{W} in the Hilbert space $L^2(\mathcal{S}^{p-1})$ such that $W_n \xrightarrow{d} \mathcal{W}$, implying $T_n(\lambda) \xrightarrow{d} \|\mathcal{W}\|^2$. The covariance kernel of \mathcal{W} is*

$$K(\mathbf{s}, \mathbf{t}) = \sum_{k=1}^{\infty} c_{k,p}(\lambda) C_k^{(p-2)/2}(\mathbf{s}^\top \mathbf{t}), \quad \mathbf{s}, \mathbf{t} \in \mathcal{S}^{p-1}. \quad (12)$$

From this result, we derive the limit distribution of the test statistic.

Theorem 3.2. *For $p \geq 2$ and under \mathcal{H}_0 we get the asymptotic distribution*

$$T_n(\lambda) \xrightarrow{d} T_\infty(\lambda) := \sum_{k=1}^{\infty} c_{k,p}(\lambda) \gamma_{k,p} Z_{d_{k,p}} \quad \text{for } n \rightarrow \infty,$$

where $Z_{d_{k,p}} \sim \chi_{d_{k,p}}^2$ are independent and $\gamma_{k,p}$ is defined in (6).

From Theorem 3.2 and the moments of independent chi-squared distributions, we derive the expectation and variance of the limiting random variable as the series expansions $\mathbb{E}_{\mathcal{H}_0} [T_\infty] = \sum_{k=1}^{\infty} c_{k,p}(\lambda) \gamma_{k,p} d_{k,p}$ and $\text{Var}_{\mathcal{H}_0} [T_\infty] = \sum_{k=1}^{\infty} 2(c_{k,p}(\lambda) \gamma_{k,p})^2 d_{k,p}$.

To compute the variance of $T_n(\lambda)$ under \mathcal{H}_0 for a fixed $n \in \mathbb{N}$, we use the variance formula for U -statistics, and the fact that we have a centered degenerate kernel and a constant diagonal, to see that the variance takes the form,

$$\text{Var}_{\mathcal{H}_0} [T_n(\lambda)] = (n-1)^2 \frac{2}{n(n-1)} \mathbb{E}_{\mathcal{H}_0} \left[\left(\sum_{k=1}^{\infty} c_{k,p}(\lambda) C_k^{(p-2)/2}(\mathbf{X}^\top \mathbf{Y}) \right)^2 \right] \quad (13)$$

$$= \sum_{k=1}^{\infty} 2 \frac{n-1}{n} (c_{k,p}(\lambda) \gamma_{k,p})^2 d_{k,p}. \quad (14)$$

3.2 Fixed alternatives

For any random vector \mathbf{X} on \mathcal{S}^{p-1} with fixed density q with respect to the uniform measure ν_{p-1} , we derive the almost sure limit of $T_n(\lambda)/n$ as well as the limit distribution of the centered test statistic. Given a general decomposition of the density, as expressed in (10) and (11), we first provide expansions of $M_{\mathbf{X}}$ and z .

Lemma 3.1. *For an absolutely continuous random vector \mathbf{X} on \mathcal{S}^{p-1} with density $q \in L^2(\mathcal{S}^{p-1})$, let $\mathbf{t} \in \mathbb{R}^p \setminus \{\mathbf{0}\}$ and $\mathbf{s} \in \mathcal{S}^{p-1}$. Then, in $L^2(\mathcal{S}^{p-1})$,*

$$M_{\mathbf{X}}(\lambda \mathbf{t}) = \sum_{k=0}^{\infty} \sum_{r=1}^{d_{k,p}} \beta_{r,k} m_{k,p}(\lambda \|\mathbf{t}\|) \gamma_{k,p} Y_{r,k} \left(\frac{\mathbf{t}}{\|\mathbf{t}\|} \right),$$

$$z(\mathbf{s}) := \Delta_{\mathcal{S}^{p-1}} M_{\mathbf{X}}(\lambda \mathbf{s}) = \sum_{k=1}^{\infty} \sum_{r=1}^{d_{k,p}} \beta_{r,k} m_{k,p}(\lambda) \gamma_{k,p} (-k)(k+p-2) Y_{r,k}(\mathbf{s}).$$

Now, by establishing the almost sure convergence $W_n/\sqrt{n} \rightarrow z$ in $L^2(\mathcal{S}^{p-1})$ and applying the representation from Lemma 3.1 in the proof in Appendix A, we obtain the almost sure limit of $T_n(\lambda)/n$ for $n \rightarrow \infty$.

Theorem 3.3. *Let $p \geq 2$ and let $\mathbf{X}_1, \dots, \mathbf{X}_n$ be iid copies of an absolutely continuous random vector \mathbf{X} on \mathcal{S}^{p-1} with density $q \in L^2(\mathcal{S}^{p-1})$. Then,*

$$\frac{T_n(\lambda)}{n} \xrightarrow{a.s.} \tau = \|z\|_{L^2(\mathcal{S}^{p-1})}^2 = \sum_{k=1}^{\infty} \sum_{r=1}^{d_{k,p}} \beta_{r,k}^2 c_{k,p}(\lambda) \gamma_{k,p}, \quad \text{as } n \rightarrow \infty.$$

Remark 3.1. *Theorem 3.3 implies consistency against all absolutely continuous non-uniform distributions. First, by the characterization in (2), $z \equiv \mathbf{0}$ if and only if \mathbf{X} is uniformly distributed on \mathcal{S}^{p-1} and thus $\tau > 0$ for all alternative distributions. This consistency is also observed in the Gegenbauer decomposition of Theorem 3.3, since $c_{k,p}(\lambda) \gamma_{k,p} > 0$ implies that, for all densities q , $z \equiv \mathbf{0}$ if and only if $\beta_{r,k} = 0$ for all $k \geq 1$, which again implies uniformity. These observations connect to Sobolev test theory (Giné, 1975, Theorem 4.4) since the coefficients $c_{k,p}(\lambda)$ are positive for all $k \in \mathbb{N}$.*

With the same arguments as in Theorem 3.3, we derive the expectation for fixed n as a series of spherical harmonics.

Remark 3.2. *As a result from the proof of Theorem 3.3, we obtain*

$$\mathbb{E}[T_n(\lambda)] = (n-1) \sum_{k=1}^{\infty} \sum_{r=1}^{d_{k,p}} \beta_{r,k}^2 c_{k,p}(\lambda) \gamma_{k,p} + \sum_{k=1}^{\infty} c_{k,p}(\lambda) C_k^{(p-2)/2}(1).$$

Focusing further on the underlying random field, we find the limit Gaussian field (after recentering by the expectation) in analogy to Theorem 3.1. We introduce the notation $\Delta_{\mathcal{S}^{p-1}, \mathbf{t}}$ to denote the Laplace–Beltrami operator on \mathcal{S}^{p-1} acting with respect to the variable $\mathbf{t} \in \mathcal{S}^{p-1}$.

Theorem 3.4. *Let $p \geq 2$ and let $\mathbf{X}_1, \dots, \mathbf{X}_n$ be iid copies of an absolutely continuous random vector \mathbf{X} on \mathcal{S}^{p-1} with density q . Then there exists a real-valued centered Gaussian random element \mathcal{W}' in $L^2(\mathcal{S}^{p-1})$ for which*

$$(W_n - \sqrt{n}z) \xrightarrow{d} \mathcal{W}'$$

holds for $n \rightarrow \infty$, and where \mathcal{W}' has the covariance kernel

$$K'(\mathbf{s}, \mathbf{t}) = \Delta_{\mathcal{S}^{p-1}, \mathbf{s}} \Delta_{\mathcal{S}^{p-1}, \mathbf{t}} M_{\mathbf{X}}(\lambda(\mathbf{s} + \mathbf{t})) - \Delta_{\mathcal{S}^{p-1}} M_{\mathbf{X}}(\lambda \mathbf{s}) \Delta_{\mathcal{S}^{p-1}} M_{\mathbf{X}}(\lambda \mathbf{t})$$

$$= \sum_{k_1=0}^{\infty} \sum_{k_2=0}^{\infty} (m_{k_1,p}(\lambda)(-k_1)(k_1+p-2))(m_{k_2,p}(\lambda)(-k_2)(k_2+p-2))\xi_{k_1,k_2}(\mathbf{s}, \mathbf{t}) - z(\mathbf{s})z(\mathbf{t}).$$

Here, we write $\xi_{k_1,k_2}(\mathbf{s}, \mathbf{t}) = \mathbb{E}[C_{k_1}^{(p-2)/2}(\mathbf{s}^\top \mathbf{X})C_{k_2}^{(p-2)/2}(\mathbf{t}^\top \mathbf{X})]$ for all $\mathbf{s}, \mathbf{t} \in \mathcal{S}^{p-1}$.

For applications, it is convenient to consider a finite-dimensional projection of the random field \mathcal{W}' to get a covariance matrix corresponding to the kernel at a fixed set of vectors on the sphere.

Remark 3.3. Let $m \in \mathbb{N}$ and fix $\mathbf{t}_1, \dots, \mathbf{t}_m \in \mathcal{S}^{p-1}$. For $k \in \mathbb{N}$, define the vectors of Gegenbauer polynomials and spherical harmonics as

$$\mathbf{C}_k(\mathbf{x}) := (C_k^{(p-2)/2}(\mathbf{t}_1^\top \mathbf{x}), \dots, C_k^{(p-2)/2}(\mathbf{t}_m^\top \mathbf{x}))^\top \text{ and } \mathbf{Y}_{r,k} := (Y_{r,k}(\mathbf{t}_1), \dots, Y_{r,k}(\mathbf{t}_m))^\top.$$

This notation allows us to write the covariance matrix \mathbf{K}_m of the Gaussian limit of the random vector $\mathbf{W}_n - \sqrt{n}\mathbf{z} := (W_n(\mathbf{t}_1) - \sqrt{n}z(\mathbf{t}_1), \dots, W_n(\mathbf{t}_m) - \sqrt{n}z(\mathbf{t}_m))^\top$, corresponding to the kernel K' in Theorem 3.4, as

$$\begin{aligned} \text{vec}(\mathbf{K}_m) &= \mathbb{E} \left[\left(\sum_{k=1}^{\infty} (m_{k,p}(\lambda)(-k)(k+p-2)) \left(\mathbf{C}_k(\mathbf{X}) - \gamma_{k,p} \sum_{r=1}^{d_{k,p}} \beta_{r,k} \mathbf{Y}_{r,k} \right) \right)^{\otimes 2} \right] \\ &= \mathbb{E} \left[\left(\sum_{k=1}^{\infty} (m_{k,p}(\lambda)(-k)(k+p-2)) \mathbf{C}_k(\mathbf{X}) \right)^{\otimes 2} \right] - \mathbf{z}^{\otimes 2}, \end{aligned}$$

where $\mathbf{z}^{\otimes 2} = \mathbf{z} \otimes \mathbf{z} = \text{vec}(\mathbf{z}\mathbf{z}^\top)$. The entries of \mathbf{K}_m are $(\mathbf{K}_m)_{i,j} = K'(\mathbf{t}_i, \mathbf{t}_j)$.

Although this representation is more practical, it cannot be expressed in closed form, as the expectation ξ_{k_1,k_2} has to be evaluated at different vectors \mathbf{s}, \mathbf{t} with $\mathbf{s} \neq \mathbf{t}$. Restricting to the case $\mathbf{s} = \mathbf{t}$, the expectation can be expressed using the linearization formula for Gegenbauer polynomials (24), leading to a closed expression for the variance function of the random field.

Remark 3.4. Looking at the variance function of \mathcal{W}' in a direction $\mathbf{s} \in \mathcal{S}^{p-1}$ with the linearization formula (24) yields the closed expression

$$\xi_{k_1,k_2}(\mathbf{s}, \mathbf{s}) = \sum_{\ell=0}^{\min(k_1,k_2)} L_{k_1,k_2}^{(p)}(\ell) \gamma_{k_1,p+k_2-2\ell} \sum_{r_3=1}^{d_{k_1,p+k_2-2\ell}} \beta_{r_3,k_1+k_2-2\ell} Y_{r_3,k_1+k_2-2\ell}(\mathbf{s}).$$

Using the limit distribution of the random field W_n in Theorem 3.4, we derive the limit distribution of the centered test statistic.

Theorem 3.5. Let $p \geq 2$ and let $\mathbf{X}_1, \dots, \mathbf{X}_n$ be iid copies of a random vector \mathbf{X} on \mathcal{S}^{p-1} with density q . Then

$$\sqrt{n} \left(\frac{T_n(\lambda)}{n} - \tau \right) \xrightarrow{d} \mathcal{N}(0, \sigma^2),$$

with

$$\begin{aligned} \sigma^2 &= 4 \int_{\mathcal{S}^{p-1}} \int_{\mathcal{S}^{p-1}} K'(\mathbf{s}, \mathbf{t}) z(\mathbf{s})z(\mathbf{t}) d\nu_{p-1}(\mathbf{s}) d\nu_{p-1}(\mathbf{t}) \\ &= 4\mathbb{E} \left[\left(\sum_{k=1}^{\infty} \sum_{r=1}^{d_{k,p}} \gamma_{k,p} C_{k,p}(\lambda) \beta_{r,k} (Y_{r,k}(\mathbf{X}) - \beta_{r,k}) \right)^2 \right]. \end{aligned}$$

3.3 Rotationally symmetric alternatives

We specialize the general alternative theory to the important class of rotationally symmetric alternatives about a fixed direction $\boldsymbol{\mu} \in \mathcal{S}^{p-1}$. The key advantage of rotational symmetry is that it allows for simplifications of the spherical harmonic decomposition. It is sufficient to decompose the density in Gegenbauer polynomials, due to the zonal structure. For a zonal density q , there is an angular function $g : [-1, 1] \rightarrow \mathbb{R}$ so that we find the Gegenbauer decomposition,

$$q(\mathbf{x}) = g(\boldsymbol{\mu}^\top \mathbf{x}) = \sum_{k=0}^{\infty} \beta_k C_k^{(p-2)/2}(\boldsymbol{\mu}^\top \mathbf{x}), \quad \beta_k = \int_{\mathcal{S}^{p-1}} q(\mathbf{x}) C_k^{(p-2)/2}(\boldsymbol{\mu}^\top \mathbf{x}) d\nu_{p-1}(\mathbf{x}).$$

As an example, we explicitly derive the coefficients β_k in closed form for for the von Mises–Fisher (vMF) distribution.

Example 3.1. Let $\kappa > 0$ and $\boldsymbol{\mu} \in \mathcal{S}^{p-1}$, and denote by $f_{\text{vMF}}(\cdot; \boldsymbol{\mu}, \kappa)$ the density of the von Mises–Fisher distribution $\text{vMF}(\boldsymbol{\mu}, \kappa)$ with respect to ν_{p-1} , so

$$f_{\text{vMF}}(\mathbf{x}; \boldsymbol{\mu}, \kappa) = \frac{\kappa^{(p-2)/2} \omega_{p-1}}{(2\pi)^{p/2} \mathcal{I}_{(p-2)/2}(\kappa)} e^{\kappa \boldsymbol{\mu}^\top \mathbf{x}}, \quad \text{for all } \mathbf{x} \in \mathcal{S}^{p-1}.$$

Combining (5) and (4), we obtain the decomposition

$$f_{\text{vMF}}(\mathbf{x}; \boldsymbol{\mu}, \kappa) = \frac{\kappa^{(p-2)/2} \omega_{p-1}}{(2\pi)^{p/2} \mathcal{I}_{(p-2)/2}(\kappa)} \sum_{k=0}^{\infty} m_{k,p}(\kappa) C_k^{(p-2)/2}(\boldsymbol{\mu}^\top \mathbf{x}).$$

This implies the Gegenbauer coefficients admit the explicit form

$$\beta_k = \frac{\kappa^{(p-2)/2} \omega_{p-1}}{(2\pi)^{p/2} \mathcal{I}_{(p-2)/2}(\kappa)} m_{k,p}(\kappa), \quad k \in \mathbb{N}_0. \quad (15)$$

The results in Lemma 3.1 and Theorem 3.3 simplify by exploiting the Gegenbauer decomposition.

Remark 3.5. Under the assumption of rotational symmetry, we find with the same arguments used in the proof of Lemma 3.1 that

$$z(\mathbf{s}) = \sum_{k=1}^{\infty} \beta_k m_{k,p}(\lambda) \gamma_{k,p}(-k) (k+p-2) C_k^{(p-2)/2}(\boldsymbol{\mu}^\top \mathbf{s}), \quad \mathbf{s} \in \mathcal{S}^{p-1}. \quad (16)$$

The limit τ as defined in Theorem 3.3, simplifies to

$$\frac{T_n(\lambda)}{n} \xrightarrow{\text{a.s.}} \tau = \sum_{k=1}^{\infty} (\beta_k \gamma_{k,p})^2 c_{k,p}(\lambda) C_k^{(p-2)/2}(1).$$

Here, the factor $\gamma_{k,p} C_k^{(p-2)/2}(1)$ arises from taking the integral with respect to ν_{p-1} of $C_k^{(p-2)/2}(\boldsymbol{\mu}^\top \mathbf{t})^2$, via the Funk–Hecke formula and exploiting the orthogonal relation of the Gegenbauer polynomials (7).

Further, the results for the random field W_n are simplified. A key advantage in these remarks is that the spherical harmonic coefficients β_k are determined in explicit form for alternatives such as the vMF distribution, so the asymptotic distribution is available without numerically approximating the coefficients $\beta_{r,k}$.

Remark 3.6. With the same notation as in Remark 3.3 we write the covariance matrix \mathbf{K}_m , corresponding to the kernel K' in Theorem 3.4, as

$$\text{vec}(\mathbf{K}_m) = \mathbb{E} \left[\left(\sum_{k=1}^{\infty} (m_{k,p}(\lambda) (-k)(k+p-2)) (\mathbf{C}_k(\mathbf{X}) - \gamma_{k,p} \beta_k \mathbf{C}_k(\boldsymbol{\mu})) \right)^{\otimes 2} \right]. \quad (17)$$

More generally, for two fixed vectors $\mathbf{s}, \mathbf{t} \in \mathcal{S}^{p-1}$, the kernel is expressed as

$$K'(\mathbf{s}, \mathbf{t}) = \sum_{k_1=0}^{\infty} \sum_{k_2=0}^{\infty} (m_{k_1,p}(\lambda)(-k_1)(k_1+p-2))(m_{k_2,p}(\lambda)(-k_2)(k_2+p-2)) \\ \times \left(\xi_{k_1,k_2}(\mathbf{s}, \mathbf{t}) - \gamma_{k_1,p} \gamma_{k_2,p} \beta_{k_1} \beta_{k_2} C_{k_1}^{(p-2)/2}(\boldsymbol{\mu}^\top \mathbf{s}) C_{k_2}^{(p-2)/2}(\boldsymbol{\mu}^\top \mathbf{t}) \right).$$

Remark 3.7. In this setting, we simplify the expression of the variance from Theorem 3.5, similar to Remark 3.6, and get

$$\sigma^2 = 4\mathbb{E} \left[\left(\sum_{k=1}^{\infty} \gamma_{k,p} c_{k,p}(\lambda) \beta_k \left(C_k^{(p-2)/2}(\boldsymbol{\mu}^\top \mathbf{X}) - \beta_k \gamma_{k,p} C_k^{(p-2)/2}(1) \right) \right)^2 \right] \\ = 4 \left(\sum_{k_1=0}^{\infty} \sum_{k_2=0}^{\infty} \gamma_{k_1,p} c_{k_1,p}(\lambda) \beta_{k_1} \gamma_{k_2,p} c_{k_2,p}(\lambda) \beta_{k_2} \sum_{\ell=0}^{\min(k_1,k_2)} \beta_{k_1+k_2-2\ell} L_{k_1,k_2}^{(p)}(\ell) \gamma_{k_1+k_2-2\ell,p} C_{k_1+k_2-2\ell}^{(p-2)/2}(1) \right. \\ \left. - \left(\sum_{k=1}^{\infty} \sum_{r=1}^{d_{k,p}} (\beta_{r,k})^2 \gamma_{k,p} c_{k,p}(\lambda) C_k^{(p-2)/2}(1) \right)^2 \right).$$

Here, the last equality holds by applying the linearization formula (24) on the polynomials $C_k^{(p-2)/2}(\boldsymbol{\mu}^\top \mathbf{X})$, yielding a closed-form expression. This expression is derived in the proof of Theorem 3.5 in Appendix A.

4 Connections to other tests

4.1 Limit behavior of the test for $\lambda \rightarrow 0$ and $\lambda \rightarrow \infty$

The power of the test based on $T_n(\lambda)$ is sensitive to different choices of λ , see Figure 5. In the following proposition, we analyze the limit behavior of the test statistic for extreme values of λ and fixed sample size n . Here, we use the stochastic Landau symbols, so $X_n = o_{\mathbb{P}}(1)$ denotes the convergence in probability of X_n to zero.

Proposition 4.1. Fix $n \in \mathbb{N}$ and $\mathbf{X}_1, \dots, \mathbf{X}_n$ iid on \mathcal{S}^{p-1} . As $\lambda \rightarrow 0$ and $\lambda \rightarrow \infty$ the rejection rule based on $T_n(\lambda)$ is asymptotically equivalent to

i. the Rayleigh (1919) test for $\lambda \rightarrow 0$, since $\lim_{\lambda \rightarrow 0} \lambda^{-2} T_n(\lambda) \propto \frac{1}{n} \sum_{i,j=1}^n \mathbf{X}_i^\top \mathbf{X}_j$;

ii. the Cai et al. (2013) test for $\lambda \rightarrow \infty$, since, for $D_n(\lambda) := \frac{1}{n} \sum_{j=1}^n \left\| \Delta_{\mathcal{S}^{p-1}} e^{\lambda \mathbf{t}^\top \mathbf{X}_j} \right\|_{L^2(\mathcal{S}^{p-1})}^2$,

$$\lim_{\lambda \rightarrow \infty} \lambda^{-1} \log (T_n(\lambda) - D_n(\lambda)) = \max_{1 \leq i < j \leq n} \mathbf{X}_i^\top \mathbf{X}_j + o_{\mathbb{P}}(1).$$

The Rayleigh limit concentrates all weight on the first-order component and is consequently non-omnibus consistent. The maximum-type limit reduces to a single extreme inner product, so it cannot be expressed as a V -statistic or U -statistic of the form (8). In contrast, for any fixed $\lambda > 0$, the representation in (9) assigns positive weight to all orders k .

This limit behavior for λ coincides with the behavior observed in the softmax test ($S_n(\kappa)$) introduced in Fernández-de-Marcos and García-Portugués (2023) with tuning parameter κ . For any fixed $\lambda = \kappa \in (0, \infty)$, the Gegenbauer coefficients of $T_n(\lambda)$ and $S_n(\lambda)$ differ by a factor of $m_{k,p}(\lambda)(k(k+p-2))^2 \gamma_{k,p}$. Since this factor decays rapidly as $k \rightarrow \infty$ for fixed λ , $T_n(\lambda)$ places the majority of its weight on a smaller range of indices k than the softmax test. Moreover, for any tuning parameters κ, λ in $(0, \infty)$, $S_n(\kappa)$ cannot be recovered from $T_n(\lambda)$, by any reparameterization of λ .

Remark 4.1. Allowing for a complex tuning parameter $\lambda \in \mathbb{C}$ links the construction to the characteristic function of the distribution, in particular for purely imaginary arguments $i\lambda$. The resulting coefficients $c_{k,p}(i\lambda)$ are obtained from the coefficients $c_{k,p}(\lambda)$, by replacing the modified Bessel function of the first kind \mathcal{I} with the Bessel function of the first kind \mathcal{J} , reflecting the oscillating structure of the characteristic function in contrast to the exponential growth of the mgf.

4.2 Connections to Sobolev tests

A very rich family of tests of uniformity on \mathcal{S}^{p-1} is given by the Sobolev tests. Multiple equivalent representations and definitions illustrate the connections to our construction. First, we can define the Sobolev tests through the harmonic decomposition of the zonal kernel, where it is again convenient that the spherical harmonics form eigenfunctions of our Stein operator.

Remark 4.2. Let $\mathbf{X}_1, \dots, \mathbf{X}_n$ iid on \mathcal{S}^{p-1} and define $\theta_{i,j} = \arccos(\mathbf{X}_i^\top \mathbf{X}_j)$. The class of Sobolev test statistics by Beran (1968), Giné (1975), and Prentice (1978) has the form

$$S_{n,p}(\{w_{k,p}\}) = \frac{1}{n} \sum_{i,j=1}^n \psi(\theta_{i,j}), \quad \psi(\theta) = \sum_{k=1}^{\infty} \frac{w_{k,p}}{\gamma_{k,p}} C_k^{(p-2)/2}(\cos \theta).$$

With representation (8), it becomes clear that $T_n(\lambda)$ is a member of the class of Sobolev test statistics, since for $\cos \theta_{i,j} = \mathbf{X}_i^\top \mathbf{X}_j$ we see that the Sobolev weights are given as

$$w_{k,p}^\lambda = \gamma_{k,p} c_{k,p}(\lambda).$$

A different view on the Sobolev test statistic considers a L^2 distance on an angular function g (Beran, 1968; Giné, 1975). Here, the Sobolev test, which is the locally most powerful rotation-invariant test for testing \mathcal{H}_0 against alternatives with density $g(\cdot^\top \boldsymbol{\mu})$, is given by

$$S_{n,p}(\{\psi\}) = \frac{1}{n} \left\| \sum_{i=1}^n g(\mathbf{X}_i^\top \cdot) - n \right\|_{L^2(\mathcal{S}^{p-1})}^2. \quad (18)$$

The connection of ψ to the Gegenbauer expansion in Remark 4.2 is

$$g(z) := 1 + \sum_{k=1}^{\infty} \frac{\sqrt{w_{k,p}}}{\gamma_{k,p}} C_k^{(p-2)/2}(z), \quad z \in [-1, 1].$$

We now obtain representations of general Sobolev tests as L^2 -Stein tests indexed by function classes $\{f_{\mathbf{t}} : \mathbf{t} \in \mathcal{S}^{p-1}\}$ more general than the exponential class. Consider a Sobolev test statistic $S_{n,p}(\{\psi\})$ with kernel $\psi(\theta) = \sum_{k=1}^{\infty} b_{k,p} C_k^{(p-2)/2}(\cos \theta)$, where $p \geq 2$ and $b_{k,p} \geq 0$. For the corresponding function class $\{f_{\mathbf{t}} : \mathbf{t} \in \mathcal{S}^{p-1}\}$ with

$$f_{\mathbf{t}}(\mathbf{x}) = \sum_{k=1}^{\infty} \frac{\sqrt{b_{k,p}}}{k(k+p-2)\sqrt{\gamma_{k,p}}} C_k^{(p-2)/2}(\mathbf{t}^\top \mathbf{x}),$$

the statistic $S_{n,p}(\{\psi\})$ admits the representation

$$S_{n,p}(\{\psi\}) = \frac{1}{n} \left\| \sum_{i=1}^n \Delta_{\mathcal{S}^{p-1}} f_{\mathbf{t}}(\mathbf{X}_i) \right\|_{L^2(\mathcal{S}^{p-1})}^2.$$

Now, for the angular function g of (18), we see $g(\mathbf{x}^\top \mathbf{t}) = 1 - \Delta_{\mathcal{S}^{p-1}} f_{\mathbf{t}}(\mathbf{x})$, using the eigenfunction relation of Gegenbauer polynomials for $\Delta_{\mathcal{S}^{p-1}}$.

4.3 Connections to the $\text{dKSD}_{(2)}^2$ test

There are different ways to define a test statistic based on a Stein operator. To contrast the proposed L^2 -Stein approach, we consider a directional kernel Stein discrepancy test with the same operator and kernel functions and compare the resulting structures. The application of a kernel Stein discrepancy (KSD) in a directional setting has been considered in Xu and Matsuda (2020). For the iid random vectors $\mathbf{X}_1, \dots, \mathbf{X}_n$ with unknown density q and target density d , with Stein operator \mathcal{A}_d , the dKSD V -statistic takes the form

$$\text{dKSD}_{(2)}^2 = \frac{1}{n^2} \sum_{i,j=1}^n h_d(\mathbf{X}_i, \mathbf{X}_j), \quad \text{where } h_d(\mathbf{x}, \mathbf{y}) = \langle \mathcal{A}_d k(\mathbf{x}, \cdot), \mathcal{A}_d k(\mathbf{y}, \cdot) \rangle_{\mathcal{H}}, \quad (19)$$

see Xu and Matsuda (2020, Equation (13)). While Xu and Matsuda (2020) uses a first-order Stein operator \mathcal{A} , here we consider the second-order Stein operator defined in (1), which we denote by the subscript (2) in (19). In Xu and Matsuda (2021), a version of KSD using a second-order Stein operator in local coordinates is discussed in a more general setting on manifolds with empty boundary.

Considering a KSD construction on the sphere and for the uniform target distribution with constant density d , we obtain the kernel

$$h_d(\mathbf{x}, \mathbf{y}) = \Delta_{S^{p-1}, \mathbf{x}} \Delta_{S^{p-1}, \mathbf{y}} k(\mathbf{x}, \mathbf{y}).$$

Here, we use the reproducing kernel property and apply the simplified operator from (1). To connect this construction to our L^2 -Stein construction, we fix the kernel to be the von Mises–Fisher kernel $k(\mathbf{x}, \mathbf{y}) = e^{\lambda \mathbf{x}^\top \mathbf{y}}$ with $\lambda > 0$. Consequently, the same Gegenbauer expansion in (5) is used to decompose the kernel, and we derive a closed Gegenbauer representation

$$\text{dKSD}_{(2)}^2 = \frac{1}{n^2} \sum_{i,j=1}^n \sum_{k=1}^{\infty} c_{k,p}^{\text{dKSD}}(\lambda) C_k^{(p-2)/2}(\mathbf{X}_i^\top \mathbf{X}_j),$$

with similar Gegenbauer coefficients $c_{k,p}^{\text{dKSD}}(\lambda) := m_{k,p}(\lambda) (k(k+p-2))^2$. This analogous representation helps identify the effect of the two constructions. It also directly allows for application of our asymptotic results from Section 3, after replacing the coefficients $c_{k,p}(\lambda)$ by $c_{k,p}^{\text{dKSD}}(\lambda)$. Hence, we provide a direct method to compute the asymptotic distribution of the test statistic, both under \mathcal{H}_0 and under fixed alternatives, incorporate the perspective of the underlying random field to analyze the test, and show that the test belongs to the class of Sobolev tests.

The coefficients of the L^2 -Stein and $\text{dKSD}_{(2)}^2$ tests differ by a factor of $c_{k,p}(\lambda)/c_{k,p}^{\text{dKSD}}(\lambda) = \gamma_{k,p} m_{k,p}(\lambda)$. To illustrate this difference, we plot standardized versions of the functions $k \mapsto c_{k,p}(\lambda)$ and $k \mapsto c_{k,p}^{\text{dKSD}}(\lambda)$ in Figure 1. The weight of the L^2 -Stein test is more concentrated on a narrow set of indices compared to the $\text{dKSD}_{(2)}^2$ test, while the concentration parameter λ has a similar effect in both approaches, shifting the weight of the tests to Gegenbauer polynomials of higher order as λ increases.

5 Numerical experiments

5.1 Visualization of covariance under alternatives

In this section, we visualize the structure of the limiting Gaussian processes obtained in Theorem 3.1 and in Theorem 3.4. These are, respectively, \mathcal{W} and \mathcal{W}' , the limit of the empirical processes $W_n - \sqrt{n}z$. To do so, we explore the shape of: (i) the centering $\mathbf{s} \mapsto \sqrt{n}z(\mathbf{s})$ under a fixed alternative ($z(\mathbf{s}) \equiv 0$ under \mathcal{H}_0); (ii) the null correlation kernel $\mathbf{s} \mapsto \rho(\mathbf{s}, \mathbf{t}) := K(\mathbf{s}, \mathbf{t})/\sqrt{K(\mathbf{s}, \mathbf{s})K(\mathbf{t}, \mathbf{t})}$; and (iii) the fixed-alternative correlation kernel $\mathbf{s} \mapsto \rho'(\mathbf{s}, \mathbf{t})$. These explorations shed light on what

parts of the sphere contribute the most to increasing the expectation of the test statistic and detect a fixed alternative, and into how the correlation structure of the random field \mathcal{W} changes into that of \mathcal{W}' .

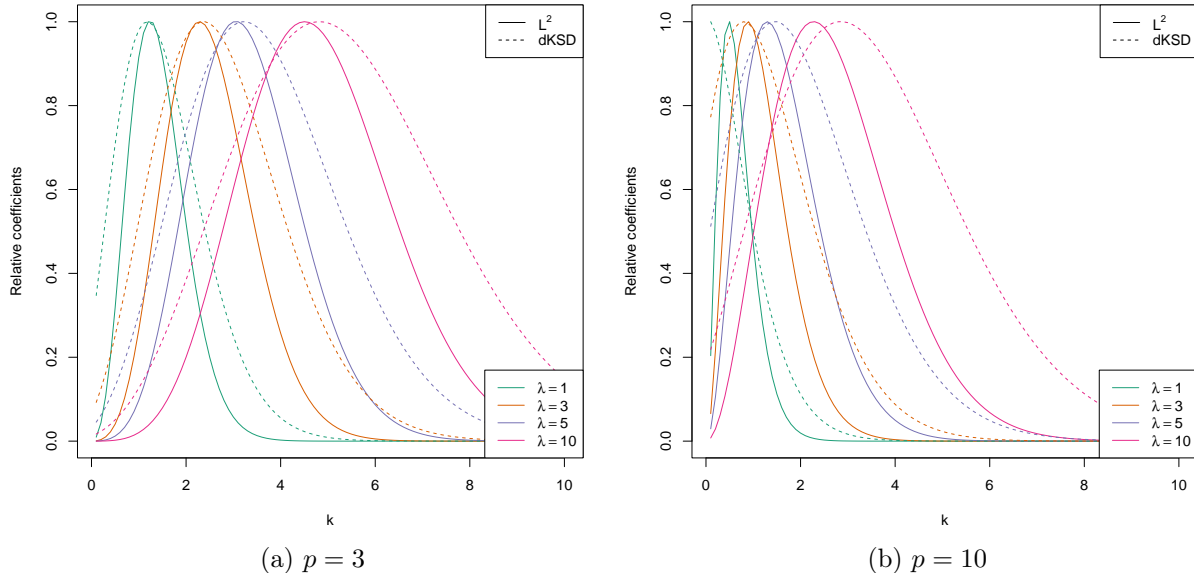


Figure 1: Relative coefficients $k \mapsto c_{k,p}(\lambda)$ and $k \mapsto c_{k,p}^{\text{dKSD}}(\lambda)$ for dimensions $p = 3$ and $p = 10$, for the L^2 -Stein test (solid lines) and the dKSD test (dashed lines). For each choice of λ , the coefficients are standardized by their maximum. To illustrate the effect, we plot the continuous mappings in k , while in the test, only evaluations at integer values of k are used.

To visualize the previous functions, we use the equal-area Hammer projection to map \mathcal{S}^2 to an elliptical projection, displaying also selected parallels and meridians. We consider the vMF($\boldsymbol{\mu}, \kappa$) distribution as a fixed alternative to leverage the expressions (16) and (17) and compute $K'(\mathbf{s}, \mathbf{t})$ and $z(\mathbf{s})$ using the explicit form for the vMF coefficients in (15). We set $\boldsymbol{\mu} = (0, -1, 0)^\top$. For computing $K(\mathbf{s}, \mathbf{t})$, we used (12). The series in $z(\mathbf{s})$, $K(\mathbf{s}, \mathbf{t})$, and $K'(\mathbf{s}, \mathbf{t})$ were truncated to their first 100 terms. To compute (17) we used Monte Carlo with $M = 10,000$ replicates.

Figure 2 shows $\mathbf{s} \mapsto \sqrt{n}|z(\mathbf{s})|$, illustrating the effects that λ and κ have on its structure. The larger λ , the larger the relative weight of $|z(\mathbf{s})|$ at about $\mathbf{s} = \boldsymbol{\mu}$ (Figure 2c), with the relative weight at the antipodal region (see Figure 2a) disappearing. This effect parallels the relative concentration effect of larger κ (Figures 2d–2f). The value of $|z(\mathbf{s})|$ at $\mathbf{s} = \boldsymbol{\mu}$ and, implied by that, the value of $\|z\|_{L^2(\mathcal{S}^{p-1})}^2$, increases monotonically with λ , as manifested in the increasing upper limits of the legends in Figures 2a–2c.

The null correlation kernel $\mathbf{s} \mapsto \rho(\mathbf{s}, \mathbf{t})$ is shown in Figure 3 for $\mathbf{t} = (0, 0, 1)^\top$. The kernel only depends on $\mathbf{s}^\top \mathbf{t}$ (i.e., it is isotropic). Increasing λ has the effect of localizing the range of the correlation kernel at $\mathbf{s} = \mathbf{t}$. This happens both for positive and negative correlations. Positive correlations are located at the northern hemisphere, for λ close to zero (Figure 3a), and then concentrate at $\mathbf{s} = \mathbf{t}$ for large λ (Figure 3c). Negative correlations are located on the southern hemisphere for small λ , but then are attracted to parallels close to the north pole for large λ . Indeed, for large λ , near-zero correlations appear at the south pole and southern hemisphere.

Finally, Figure 4 shows the fixed-alternative correlation kernel $\mathbf{s} \mapsto \rho'(\mathbf{s}, \mathbf{t})$, now dependent on $(\mathbf{s}^\top \mathbf{t}, \boldsymbol{\mu}^\top \mathbf{s}, \boldsymbol{\mu}^\top \mathbf{t})$, for $\boldsymbol{\mu} = (0, -1, 0)^\top$ and $\mathbf{t} = (0, 0, 1)^\top$. For $\kappa = 1$, the non-isotropy is subtle, with the effects of $\boldsymbol{\mu}$ being very mild, and the correlations resemble those in Figure 3. The non-isotropy becomes evident for $\kappa = 10$, where $\boldsymbol{\mu}$ affects the correlation field with the field value at \mathbf{s} depending on the angle between \mathbf{s} and $\boldsymbol{\mu}$. Strong positive correlations are still maintained at $\mathbf{s} = \mathbf{t}$, as expected.

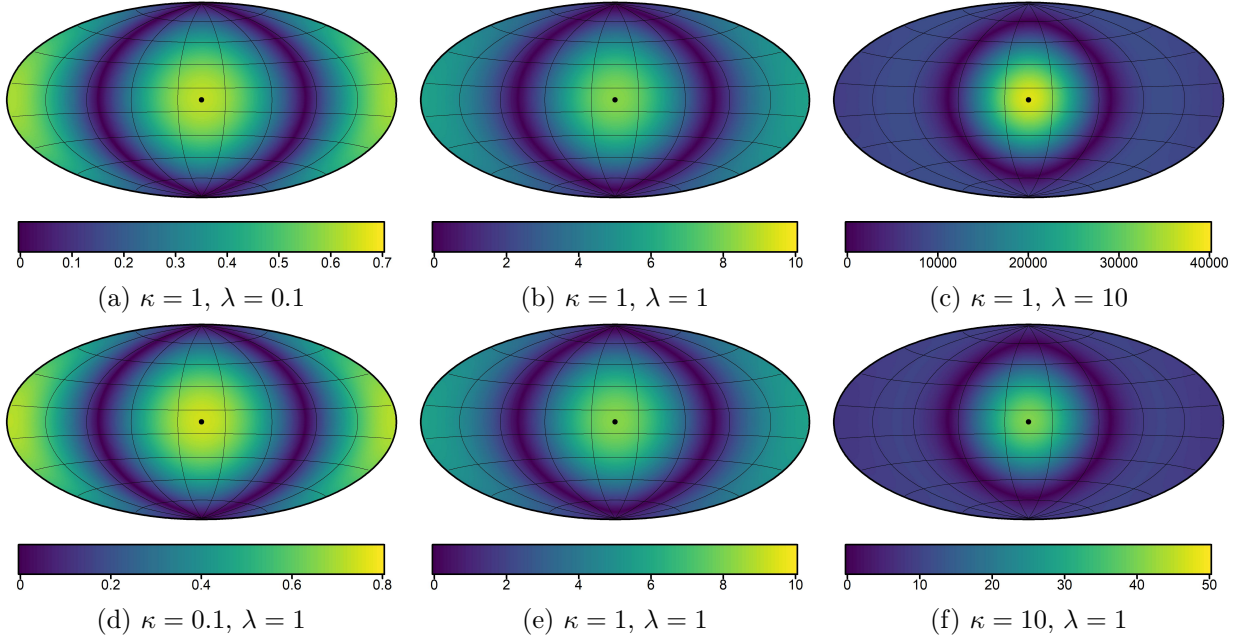


Figure 2: Hammer projection representation of $\mathbf{s} \mapsto \sqrt{n}|z(\mathbf{s})|$, for the fixed alternative $\text{vMF}(\boldsymbol{\mu}, \kappa)$ and $n = 100$. The central point is $\boldsymbol{\mu} = (0, -1, 0)^\top$. In the first row, $\kappa = 1$ is fixed, while in the second, $\lambda = 1$ is.

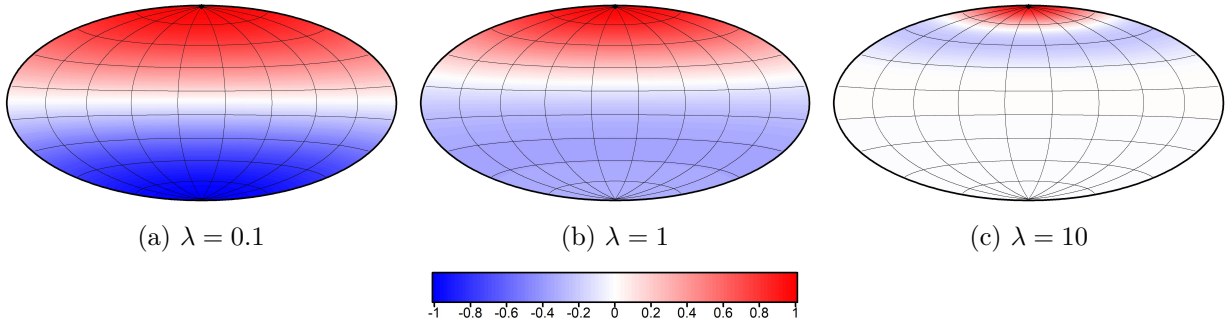


Figure 3: Hammer projection representation of the null correlation kernel $\mathbf{s} \mapsto \rho(\mathbf{s}, \mathbf{t})$, for $\mathbf{t} = (0, 0, 1)^\top$ (north pole, diamond). The shape of the kernel is invariant from the choice of \mathbf{t} .

5.2 Parameter selection

The testing procedure can be adapted to a specific alternative by selecting the tuning parameter λ that maximizes the rejection rate under the underlying distribution. To optimize the parameter λ we consider the standardized mean shift under \mathcal{H}_1 , compared to \mathcal{H}_0 :

$$\hat{\lambda} = \arg \max_{\lambda > 0} q_\lambda = \arg \max_{\lambda > 0} \frac{\mathbb{E}_{\mathcal{H}_1}[T_n(\lambda)] - \mathbb{E}_{\mathcal{H}_0}[T_n(\lambda)]}{\sqrt{\text{Var}_{\mathcal{H}_0}[T_n(\lambda)]}}.$$

Maximizing this expression corresponds to maximizing the rejection rate for a given alternative; see Gregory (1977). Here, we approximate the expectation $\mathbb{E}_{\mathcal{H}_1}[T_n(\lambda)]$ with the observed value of $T_n(\lambda)$, while (14) provides closed expressions for $\mathbb{E}_{\mathcal{H}_0}[T_n(\lambda)]$ and $\text{Var}_{\mathcal{H}_0}[T_n(\lambda)]$.

Alternatively, using Theorem 3.5 and incorporating the critical value $c_n(\lambda)$, an estimate of the power function (see Baringhaus et al. (2017, Section 3.2)) can be obtained as

$$\mathbb{P}_{\mathcal{H}_1}(T_n(\lambda) > c_n(\lambda)) \approx 1 - \Phi\left(\frac{\sqrt{n}}{\sigma}\left(\frac{c_n(\lambda)}{n} - \tau\right)\right).$$

For simplified computation, we use the score function q_λ .

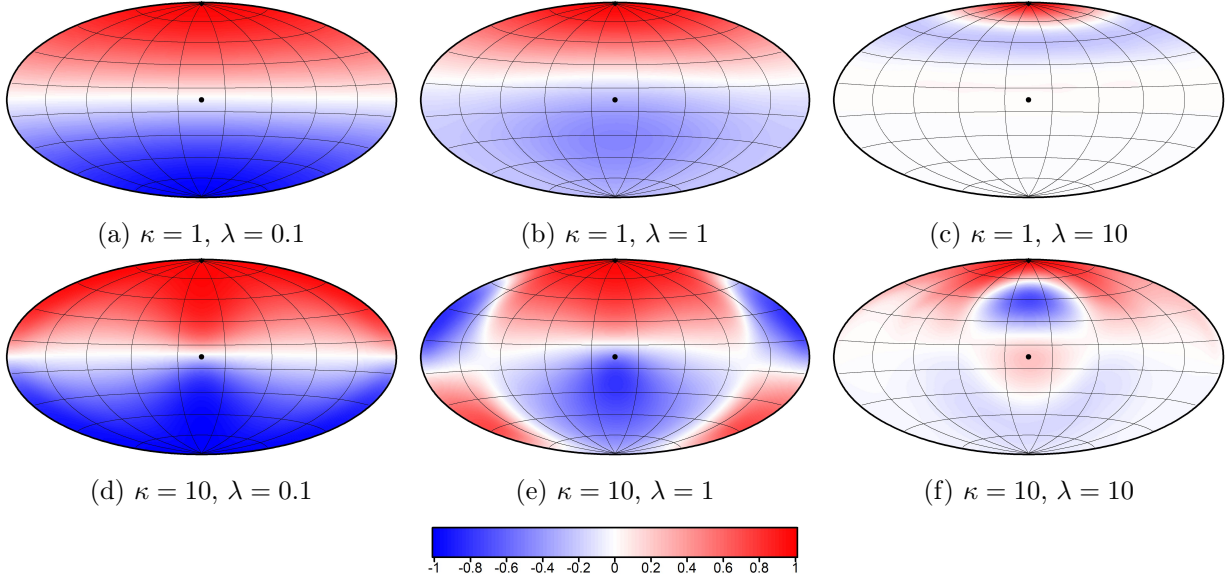


Figure 4: Hammer projection representation of the fixed-alternative correlation kernel $\mathbf{s} \mapsto \rho'(\mathbf{s}, \mathbf{t})$, for the fixed alternative vMF($\boldsymbol{\mu}, \kappa$) and $\mathbf{t} = (0, 0, 1)^\top$ (north pole, diamond). The central point is $\boldsymbol{\mu} = (0, -1, 0)^\top$.

The concentration parameter λ only affects the test statistic through the coefficients $c_{k,p}(\lambda)$. To efficiently compute the test statistic for a wide range of λ values, it is convenient to rearrange the summation to

$$T_n(\lambda) = \sum_{k=1}^{\infty} c_{k,p}(\lambda) A_k, \quad A_k = \frac{1}{n} \sum_{i,j=1}^n C_k^{(p-2)/2}(\mathbf{X}_i^\top \mathbf{X}_j),$$

with A_k independent of λ .

Now, to estimate the expectation of the test statistic $\mathbb{E}[T_n(\lambda)] = \sum_{k=1}^{\infty} c_{k,p}(\lambda) \mathbb{E}[A_k]$ for any λ , we estimate $\mathbb{E}[A_k] = (n-1) \mathbb{E}[C_k^{(p-2)/2}(\mathbf{X}_1^\top \mathbf{X}_2)] + C_k^{(p-2)/2}(1)$. Given an iid sample $\mathbf{Y}_1, \dots, \mathbf{Y}_N$, $N \in \mathbb{N}$, distributed as \mathbf{X} , this allows us to compute an approximation of $\mathbb{E}[A_k]$,

$$\bar{A}_k = (n-1) \frac{1}{N(N-1)} \sum_{1 \leq i \neq j \leq N} C_k^{(p-2)/2}(\mathbf{Y}_i^\top \mathbf{Y}_j) + C_k^{(p-2)/2}(1)$$

once in advance, to then allow for direct evaluation of the test statistic depending on λ . Then with $\bar{T}_n(\lambda) = \sum_{k=1}^{\infty} c_{k,p}(\lambda) \bar{A}_k$, we define

$$\tilde{\lambda} = \arg \max_{\lambda > 0} \frac{\bar{T}_n(\lambda) - \mathbb{E}_{\mathcal{H}_0}[T_n(\lambda)]}{\sqrt{\text{Var}_{\mathcal{H}_0}[T_n(\lambda)]}}. \quad (20)$$

Note that this approach yields an approximate choice of the tuning parameter, which relies on an independent sample from the alternative distribution. In the following section, we implement this selection approach by searching λ over the grid $\{i/10 : i \in \{1, \dots, 300\}\}$. To approximate the required coefficients, we use 10,000 independent draws from the candidate density q . For many rotationally symmetric alternatives, the coefficients β_k admit closed-form expressions, for known distributions, see Example 3.1 for the von Mises–Fisher distribution. The corresponding expectation can then be derived using Remark 3.2.

In practice, however, independent sampling from the underlying alternative is unavailable, so these quantities must be estimated from the observed data. A standard approach is cross-validation, for which we refer to the procedure described in Fernández-de-Marcos and García-Portugués (2023, Section 4). In Table 1, we compare the rejection rate of the oracle parameter test with the K -fold test, depending only on the observations. Here we use alternatives described in the following subsection.

Test	vMF(0.5)		W(1)		SC(0.5)		MvMF(5)	
	50	100	50	100	50	100	50	100
$T_n(\tilde{\lambda})$	36.52	65.10	31.78	62.42	26.58	55.22	17.22	32.14
$T_{n,20}(\lambda)$	23.90	53.38	17.46	38.10	17.94	44.70	9.28	17.90

Table 1: Empirical rejection rates in $p = 3$ with $M = 5,000$ Monte Carlo samples at significance level $\alpha = 5\%$ of the oracle parameter test $T_n(\tilde{\lambda})$ and the 20-fold cross-validation test $T_{n,20}(\lambda)$. Sample sizes are 50 and 100.

5.3 Comparison to other tests

In the following, we compare the power of the proposed test statistic against a selection of alternative distributions and benchmark it against different Sobolev tests of uniformity. To that end, we consider the test statistic $T_n(\tilde{\lambda})$ with the optimized parameter $\tilde{\lambda}$ defined in (20), and the test statistic $T_n(\lambda)$ for fixed values $\lambda \in \{1, 4\}$. The tests considered in the comparison are the Giné (1975) F_n test (F_n), the Bingham (1974) test (B_n), the Rayleigh (1919) test (R_n), the softmax test (S_n) from Fernández-de-Marcos and García-Portugués (2023), and the Projected Anderson–Darling test (PAD) from García-Portugués et al. (2023). The comparison is performed for dimensions $p = 2, 3, 5$ and sample sizes $n = 50$ and $n = 100$.

We structure the comparison by first considering unimodal alternatives. Here, we set $\boldsymbol{\mu} := \mathbf{e}_1$ with a von Mises–Fisher distribution $f_{\text{vMF}}(\mathbf{x}; \boldsymbol{\mu}, \kappa) \propto e^{\kappa \boldsymbol{\mu}^\top \mathbf{x}}$ with concentration parameter $\kappa = 0.5$ and a Cauchy-like distribution

$$f_{\text{Ca}}(\mathbf{x}; \boldsymbol{\mu}, \kappa) = \left(\frac{1 - \rho(\kappa)^2}{1 - 2\boldsymbol{\mu}^\top \mathbf{x} \rho(\kappa) + \rho(\kappa)^2} \right)^p \quad \text{with} \quad \rho(\kappa) = \frac{2\kappa + 1 - \sqrt{4\kappa + 1}}{2\kappa}, \quad \mathbf{x} \in \mathcal{S}^{p-1},$$

with concentration parameter $\kappa = 0.25$. We denote these alternatives by vMF(0.5) and Ca(0.25), respectively.

Next axial data is considered. On the one hand, we sample from the Watson distribution $f_{\text{W}}(\mathbf{x}; \boldsymbol{\mu}, \kappa) \propto e^{\kappa(\boldsymbol{\mu}^\top \mathbf{x})^2}$ with $\kappa = 1$ (denoted W(1)). On the other hand from an unbalanced mixture of two von Mises–Fisher distributions vMF(2, \mathbf{e}_1) and vMF(2, $-\mathbf{e}_1$), at opposite poles,

$$f_{\text{vMFM}}(\mathbf{x}; q) = (1 - q)f_{\text{vMF}}(\mathbf{x}; \mathbf{e}_1, 2) + qf_{\text{vMF}}(\mathbf{x}; -\mathbf{e}_1, 2), \quad \mathbf{x} \in \mathcal{S}^{p-1},$$

with $q = 0.3$ (vMFM(0.3)).

A small circle distribution $f_{\text{SC}}(\mathbf{x}; \kappa, \nu) \propto e^{-\kappa(\mathbf{e}_1^\top \mathbf{x} - \nu)^2}$, concentrated around a modal lower dimensional subsphere, with $\kappa = 0.5$ and $\nu = 0.5$ is also considered (SC(0.5, 0.5)).

To define alternatives obtained by rotating rotationally symmetric distributions, let $\mathbf{R}_{i,j}(\alpha)$ denote the rotational matrix in the (i, j) -plane with rotation angle α . With SCM(3), we denote a distribution of $k = 3$ uniformly weighted copies of distributions SC(10, 0), rotated by an angle $(j/k)2\pi$ for $j \in [k]$ in the $(2, 3)$ -plane:

$$f_{\text{SCM}}(\mathbf{x}; k) = \sum_{j=1}^k \frac{1}{k} f_{\text{SC}} \left(\mathbf{R}_{2,3} \left(-\frac{j}{k} 2\pi \right) \mathbf{x}; 10, 0 \right), \quad \mathbf{x} \in \mathcal{S}^{p-1}.$$

Analogously, projNM(5) denotes a mixture of k uniformly weighted rotated copies of a projected normal distribution. In each sample, we generate from $\mathcal{N}(4\mathbf{e}_1, \boldsymbol{\Sigma})$ with the diagonal covariance matrix $\boldsymbol{\Sigma} = \mathbf{I}_d + 9\mathbf{e}_d$, the resulting vectors are projected onto the unit sphere and rotated. First, we define the density of the projected normal distribution

$$f_{\text{projN}}(\mathbf{x}) \propto \int_0^\infty r^{p-1} \exp \left(-\frac{1}{2} (r\mathbf{x} - 4\mathbf{e}_1)^\top \boldsymbol{\Sigma} (r\mathbf{x} - 4\mathbf{e}_1) \right) dr, \quad \mathbf{x} \in \mathcal{S}^{p-1},$$

to then obtain the density of the mixture of rotated projected normal distributions, as

$$f_{\text{projNM}}(\mathbf{x}) = \sum_{j=1}^k \frac{1}{k} f_{\text{projN}} \left(\mathbf{R}_{1,2} \left(-\frac{j}{k} 2\pi \right) \mathbf{x} \right), \quad \mathbf{x} \in \mathcal{S}^{p-1}.$$

At last, with $\text{MvMF}(30)$ we denote a distribution consisting of an equal mixture of $2p$ vMF distributions with equal concentration parameter $\kappa = 30$. Here, the mean directions are the canonical unit vectors and their negatives:

$$f_{\text{MvMF}}(\mathbf{x}) = \frac{1}{2p} \sum_{j=1}^p \{f_{\text{vMF}}(\mathbf{x}; \mathbf{e}_j, \kappa) + f_{\text{vMF}}(\mathbf{x}; -\mathbf{e}_j, \kappa)\}, \quad \mathbf{x} \in \mathcal{S}^{p-1}.$$

The results are summarized in Tables 2–4. The rejection rates are computed from $M = 10,000$ Monte Carlo repetitions, with critical values under \mathcal{H}_0 at significance level $\alpha = 5\%$ approximated with M samples under the null hypothesis. For each alternative, we highlight the test statistic with the highest power as well as any tests whose power is not significantly smaller than the best-performing test in bold. Statistical significance is assessed using a paired one-sided t -test at level 5%.

Distribution	n	$T_n(\tilde{\lambda})$	$T_n(1)$	$T_n(4)$	dKSD	F_n	B_n	R_n	S_n	PAD
Unif(\mathcal{S}^{p-1})	50	5.0	5.0	5.0	5.0	5.0	5.0	5.0	5.0	5.0
	100	5.0	5.0	5.0	5.0	5.0	5.0	5.0	5.0	5.0
vMF(0.5)	50	58.1	48.6	8.2	56.1	56.0	5.9	58.1	57.5	56.7
	100	89.0	81.5	11.0	87.7	87.8	6.2	89.0	88.5	88.0
Ca(0.25)	50	32.1	26.1	6.9	31.1	31.1	5.8	32.0	31.9	31.5
	100	58.8	48.0	7.7	56.9	57.0	6.1	58.9	58.1	57.5
W(1)	50	55.3	45.5	36.7	24.7	22.8	58.3	5.4	11.7	16.8
	100	84.9	77.6	70.1	54.1	50.9	87.8	5.4	25.1	38.0
SC(0.5, 0.5)	50	50.0	46.4	11.1	50.3	50.3	12.4	47.9	49.8	50.1
	100	82.6	81.3	19.5	84.5	84.4	20.8	80.6	83.3	83.6
projNM(5)	50	11.5	5.0	6.2	5.0	5.0	4.9	4.8	4.9	5.2
	100	18.5	4.8	7.0	5.1	5.5	5.1	5.1	5.0	5.6
MvMF(30)	50	100.0	7.9	100.0	10.3	52.6	6.8	5.2	6.3	75.5
	100	100.0	8.3	100.0	16.8	100.0	7.3	5.0	6.8	100.0
vMFM(0.3)	50	93.5	93.2	69.2	87.9	88.1	84.8	68.2	82.5	85.5
	100	99.9	99.9	97.1	99.7	99.7	99.1	93.3	99.0	99.4

Table 2: Empirical rejection percentages in dimension $p = 2$ computed with $M = 10,000$ Monte Carlo samples and at significance level $\alpha = 5\%$. Bold entries indicate best-performing tests for each alternative.

We make the following observations. In the case of unimodal alternatives in all dimensions, the default parameter $\lambda = 1$ leads to similar results to the optimal choice of the Rayleigh test. The optimal $\tilde{\lambda}$ is as small as possible, achieving a rejection rate arbitrarily close to the limiting Rayleigh test, see Proposition 4.1. Using $\lambda = 4$ substantially reduces power, illustrating that larger values of λ are suboptimal against weakly concentrated alternatives. The rates for the alternative $\text{SC}(0.5, 0.5)$ behave similarly to the unimodal ones, but the optimal $\tilde{\lambda}$ does not approach zero.

In the axial alternatives, the Bingham test performs best against $W(1)$. But with optimal tuning, while $T_n(\tilde{\lambda})$ does not reach the same power as the Bingham test, it is more sensitive than the other tests considered. The $\text{vMFM}(0.3)$ alternative, with modes at opposite poles with different weights, reduces the advantage of the Bingham test, while improving detection rates for the other tests considered. In this mixed scenario, our test benefits from its flexibility. In $p = 2$ the parameter

$\lambda = 1$ performs well, while in $p = 5$, $\lambda = 4$ produces higher rejection rates than the competitors. In the case of SCM(3), there again is a lot of weight near opposing poles, but there is further concentration around small circles. Thus, the tests presented are all sensitive to the alternative, but $T_n(\tilde{\lambda})$ leads among the tests considered in this setting.

For mixtures with multiple modes of high concentration, a larger tuning parameter is preferable. As observed in Figures 3, an increasing parameter λ has a localizing effect, improving the detection of high concentration modes and preventing cancellation between opposing modes. This is evident in MvMF(30) and, in lower-dimensional settings, in projNM(5), where $T_n(\tilde{\lambda})$ and $T_n(4)$ have the highest rejection rates, while most other tests show substantially lower power.

Distribution	n	$T_n(\tilde{\lambda})$	$T_n(1)$	$T_n(4)$	dKSD	F_n	B_n	R_n	S_n	PAD
Unif(\mathcal{S}^{p-1})	50	5.0	5.0	5.0	5.0	5.0	5.0	5.0	5.0	5.0
	100	5.0	5.0	5.0	5.0	5.0	5.0	5.0	5.0	5.0
vMF(0.5)	50	35.8	34.6	8.8	33.1	35.2	5.2	35.8	35.6	35.3
	100	66.5	64.6	13.2	62.3	65.6	5.8	66.6	66.3	66.2
Ca(0.25)	50	40.2	39.0	10.6	37.8	39.7	6.6	40.4	40.2	39.9
	100	72.0	70.2	16.3	68.2	71.0	7.5	72.0	71.5	71.4
W(1)	50	32.6	13.6	26.9	17.9	10.5	37.6	5.3	8.9	9.1
	100	62.5	29.3	52.6	36.5	20.2	68.9	5.7	15.6	16.1
SC(0.5, 0.5)	50	29.1	28.8	10.0	28.4	28.9	8.1	28.6	29.2	29.1
	100	57.4	57.6	15.4	56.0	57.8	11.0	56.1	57.9	57.9
projNM(5)	50	69.8	7.3	19.1	8.7	7.9	14.3	5.3	6.4	7.7
	100	98.8	10.0	40.3	12.8	11.7	25.7	5.3	7.6	11.4
MvMF(30)	50	100.0	6.3	100.0	17.5	35.2	8.8	5.0	6.4	39.3
	100	100.0	7.3	100.0	38.5	97.1	9.3	5.5	8.6	99.5
vMFM(0.3)	50	78.9	72.4	57.7	74.7	68.5	64.1	55.0	65.8	66.0
	100	98.4	97.3	91.6	97.8	95.8	93.2	86.1	94.6	94.7
SCM(3)	50	66.5	48.0	62.0	55.3	43.4	56.2	24.1	37.7	39.8
	100	96.0	87.4	94.6	91.8	84.8	89.2	48.6	77.8	81.5

Table 3: Empirical rejection percentages in dimension $p = 3$ computed with $M = 10,000$ Monte Carlo samples and at significance level $\alpha = 5\%$. Bold entries indicate best-performing tests for each alternative.

Overall, while $T_n(\lambda)$ is omnibus consistent for all $\lambda > 0$, an appropriate choice of tuning parameter substantially improves rejection rates. The tuned test consistently leads or matches the best competitor across most settings, with W(1) as the only exception. The advantage is most pronounced for multimodal and mixture alternatives. Figure 5 illustrates the sensitivity to λ in comparison to the softmax test (Fernández-de-Marcos and García-Portugués, 2023), as well as the dKSD test discussed in Section 4.3, using the same tuning parameter λ in each test statistic. The proposed test has a narrower range of near-optimal parameters, but achieves the highest rejection rates, with optimal λ , in the alternatives considered.

6 Discussion

We introduced an L^2 -Stein test statistic in the sense of Anastasiou et al. (2023, Section 5.2) for testing uniformity on the sphere. A key feature of our approach is the dual role of the Laplace–Beltrami operator, as both the Stein operator for uniformity and an operator whose eigenfunctions are the spherical harmonics, allowing for elegant, explicit series representations of both the statistic and its asymptotic null and non-null distributions.

We finalize the paper by pointing out some extensions for further research. Within the spherical uniformity setting, one may generalize the procedure by either changing the set of test functions or by applying a different norm to the underlying process to further adapt the sensitivity profiles. Extending the setting beyond the sphere, the derived Stein operator applies for general smooth compact manifolds with empty boundary, so the construction (3) still applies. In that setting, Laplace–Beltrami eigenfunctions still yield an orthogonal basis but, in general, we lose the explicit harmonic decomposition of the test functions and the use of the Funk–Hecke theorem to derive the coefficients. The approach also allows for goodness of fit tests for other distributions than the uniform by applying the operator as stated in (1). In this more general scenario, one must additionally account for unknown model parameters that have to be estimated, and the resulting operator no longer admits a spherical-harmonic eigenbasis. As a result, the explicit harmonic decomposition available under uniformity is generally lost.

	n	$T_n(\tilde{\lambda})$	$T_n(1)$	$T_n(4)$	dKSD	F_n	B_n	R_n	S_n	PAD
Unif(\mathcal{S}^{p-1})	50	5.0	5.0	5.0	5.0	5.0	5.0	5.0	5.0	5.0
	100	5.0	5.0	5.0	5.0	5.0	5.0	5.0	5.0	5.0
vMF(0.5)	50	17.8	17.8	8.8	17.5	17.6	5.6	17.7	17.7	17.8
	100	36.1	35.9	14.1	34.5	35.5	6.1	36.1	35.8	35.8
Ca(0.25)	50	53.1	53.1	21.7	52.8	52.9	6.8	52.7	53.0	53.1
	100	86.8	86.6	45.1	84.6	86.3	9.3	86.7	86.5	86.6
W(1)	50	13.1	6.1	12.6	7.2	6.3	15.1	5.1	6.2	6.0
	100	22.2	7.1	21.6	9.3	7.6	28.8	5.3	7.4	7.0
SC(0.5, 0.5)	50	15.6	15.4	8.5	15.5	15.5	6.0	15.6	15.5	15.6
	100	29.2	29.3	12.7	28.2	29.0	7.0	29.0	29.1	29.2
projNM(5)	50	100.0	82.5	100.0	100.0	98.7	100.0	7.5	94.4	84.0
	100	100.0	100.0	100.0	100.0	100.0	100.0	7.6	100.0	100.0
MvMF(30)	50	100.0	5.2	99.9	10.2	18.7	10.1	5.0	6.3	18.0
	100	100.0	5.8	100.0	16.4	48.7	10.9	5.2	8.5	46.7
vMFM(0.3)	50	48.6	40.7	37.7	45.4	41.8	31.8	36.2	41.4	40.5
	100	82.5	74.4	72.7	77.2	75.2	62.0	66.6	75.0	73.7
SCM(3)	50	98.5	82.3	97.4	93.4	87.4	86.8	62.7	85.3	83.4
	100	100.0	100.0	100.0	100.0	100.0	100.0	98.8	100.0	100.0

Table 4: Empirical rejection percentages in dimension $p = 5$ computed with $M = 10,000$ Monte Carlo samples and at significance level $\alpha = 5\%$. Bold entries indicate best-performing tests for each alternative.

Acknowledgments

The first two authors are funded by the Deutsche Forschungsgemeinschaft (DFG, German Research Foundation), grant 541565572. The third author acknowledges support from grant PCI2024-155058-2, funded by MICIU/AEI/10.13039/501100011033/UE.

References

Anastasiou, A., Barp, A., Briol, F.-X., Ebner, B., Gaunt, R. E., Ghaderinezhad, F., Gorham, J., Gretton, A., Ley, C., Liu, Q., Mackey, L., Oates, C. J., Reinert, G., and Swan, Y. (2023). Stein’s method meets computational statistics: A review of some recent developments. *Stat. Sci.*, 38(1):120–139.

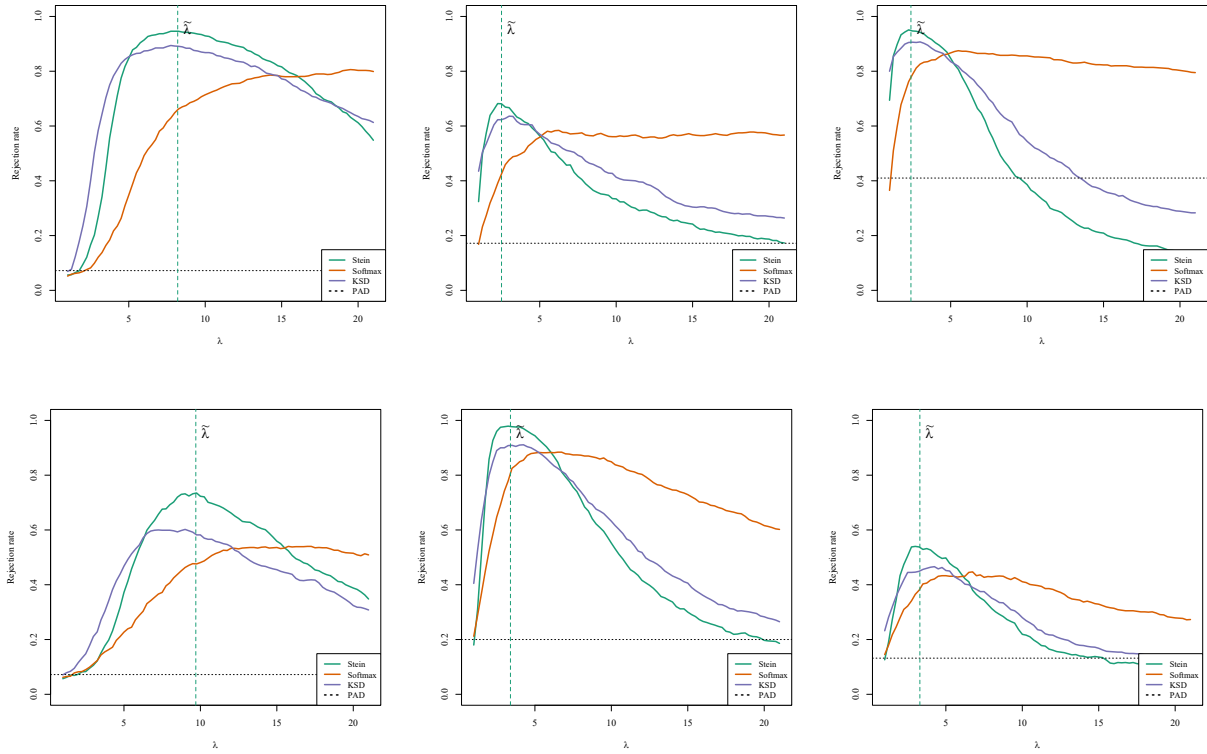


Figure 5: Powers of Stein, softmax tests, and dKSD test, with concentration parameter λ in each column under the alternative distributions MvMF(10), SCM(3), and W(2). In the top row, the simulation was carried out in dimension $p = 3$ while the bottom row was carried out in dimension $p = 5$. Here, we use significance level $\alpha = 5\%$, sample size $n = 50$, and $M = 1,000$ samples.

Barbour, A. D. (1988). Stein’s method and Poisson process convergence. *J. Appl. Probab.*, 25(A):175–184.

Barbour, A. D. (1990). Stein’s method for diffusion approximations. *Probab. Theory Relat. Fields*, 84(3):297–322.

Baringhaus, L., Ebner, B., and Henze, N. (2017). The limit distribution of weighted L^2 -goodness-of-fit statistics under fixed alternatives, with applications. *Ann. Inst. Stat. Math.*, 69(5):969–995.

Barp, A., Oates, C. J., Porcu, E., and Girolami, M. (2022). A Riemann–Stein kernel method. *Bernoulli*, 28(4):2181–2208.

Beran, R. J. (1968). Testing for uniformity on a compact homogeneous space. *J. Appl. Probab.*, 5(1):177–195.

Bingham, C. (1974). An antipodally symmetric distribution on the sphere. *Ann. Stat.*, 2(6):1201–1225.

Borodavka, J. I. and Ebner, B. (2026). A general maximal projection approach to uniformity testing on the hypersphere. *Bernoulli*, 32(2):996 – 1019.

Cai, T., Fan, J., and Jiang, T. (2013). Distributions of angles in random packing on spheres. *J. Mach. Learn. Res.*, 14(21):1837–1864.

Chen, L. H. Y., Goldstein, L., and Shao, Q.-M. (2011). *Normal Approximation by Stein’s Method*. Springer, Berlin, Heidelberg.

- Cutting, C., Paindaveine, D., and Verdebout, T. (2017). Testing uniformity on high-dimensional spheres against monotone rotationally symmetric alternatives. *Ann. Stat.*, 45(3):1024–1058.
- Dai, F. and Xu, Y. (2013). *Approximation Theory and Harmonic Analysis on Spheres and Balls*. Springer Monographs in Mathematics. Springer, New York.
- Ding, Y., Markatou, M., and Saraceno, G. (2025). Poisson kernel-based tests for uniformity on the d -dimensional sphere. *Stat. Sin.*, 35(4):1947–1969.
- DLMF (2020). *NIST Digital Library of Mathematical Functions*. <http://dlmf.nist.gov/>, Release 1.0.27 of 2020-06-15. F. W. J. Olver, A. B. Olde Daalhuis, D. W. Lozier, B. I. Schneider, R. F. Boisvert, C. W. Clark, B. R. Miller and B. V. Saunders, eds.
- Ebner, B., García-Portugués, E., and Verdebout, T. (2025). High-dimensional Sobolev tests on hyperspheres. *arXiv:2501.10898*.
- Fernández-de-Marcos, A. and García-Portugués, E. (2023). On new omnibus tests of uniformity on the hypersphere. *Test*, 32(4):1508–1529.
- Fischer, A., Gaunt, R. E., and Swan, Y. (2026). Stein’s method of moments on the sphere. *Bernoulli*, 32(2):1186–1212.
- García-Portugués, E., Navarro-Esteban, P., and Cuesta-Albertos, J. A. (2023). On a projection-based class of uniformity tests on the hypersphere. *Bernoulli*, 29(1):181–204.
- García-Portugués, E., Paindaveine, D., and Verdebout, T. (2026). On a class of Sobolev tests for symmetry, their detection thresholds, and asymptotic powers. *To appear: J. Am. Stat. Assoc.*
- García-Portugués, E. and Verdebout, T. (2018). A review of uniformity tests on the hypersphere. *arXiv:1804.00286*.
- Giné, E. (1975). Invariant tests for uniformity on compact Riemannian manifolds based on Sobolev norms. *Ann. Stat.*, 3(6):1243–1266.
- Gregory, G. G. (1977). Large sample theory for U -statistics and tests of fit. *Ann. Stat.*, 5(1):110–123.
- Henze, N. (2024). *Asymptotic Stochastics: An Introduction with a View towards Statistics*, volume 10 of *Mathematics Study Resources*. Springer, Berlin, Heidelberg.
- Hsu, E. P. (2002). *Stochastic Analysis on Manifolds*, volume 38 of *Graduate Studies in Mathematics*. American Mathematical Society.
- Kalf, H. (1995). On the expansion of a function in terms of spherical harmonics in arbitrary dimensions. *Bull. Belg. Math. Soc. Simon Stevin*, 2(4):361–380.
- Ley, C. and Verdebout, T. (2017). *Modern Directional Statistics*. Chapman & Hall/CRC Interdisciplinary Statistics Series. CRC Press, Boca Raton.
- Linnik, Y. V. (1953a). Linear forms and statistical criteria. I. *Ukrainskii Matematicheskii Zhurnal*, 5:207–243. In Russian.
- Linnik, Y. V. (1953b). Linear forms and statistical criteria. II. *Ukrainskii Matematicheskii Zhurnal*, 5:247–290. In Russian.
- Mardia, K. V. and Jupp, P. E. (1999). *Directional Statistics*. Wiley Series in Probability and Statistics. Wiley, Chichester.

- Nikitin, Y. Y. (2017). Tests based on characterizations, and their efficiencies: A survey. *Acta Comment. Univ. Tartu. Math.*, 21(1):34–55.
- Pewsey, A. and García-Portugués, E. (2021). Recent advances in directional statistics. *Test*, 30(1):1–58.
- Prentice, M. J. (1978). On invariant tests of uniformity for directions and orientations. *Ann. Stat.*, 6(1):169–176.
- Qu, X. and Vemuri, B. C. (2025). Theory and applications of kernel Stein’s method on Riemannian manifolds. *arXiv:2501.00695*.
- Rayleigh, Lord. (1919). On the problem of random vibrations, and of random flights in one, two, or three dimensions. *Lond. Edinb. Dublin Philos. Mag. J. Sci.*, 37(220):321–347.
- Stein, C. M. (1972). A bound for the error in the normal approximation to the distribution of a sum of dependent random variables. In *Proceedings of the Sixth Berkeley Symposium on Mathematical Statistics and Probability (Univ. California, Berkeley, Calif., 1970/1971), Vol. II: Probability theory*, pages 583–602. Univ. California Press, Berkeley, CA.
- Xu, W. and Matsuda, T. (2020). A Stein goodness-of-fit test for directional distributions. In *Proceedings of the Twenty Third International Conference on Artificial Intelligence and Statistics*, volume 108 of *Proceedings of Machine Learning Research*, pages 320–330. PMLR.
- Xu, W. and Matsuda, T. (2021). Interpretable Stein goodness-of-fit tests on Riemannian manifold. In *Proceedings of the 38th International Conference on Machine Learning*, volume 139 of *Proceedings of Machine Learning Research*, pages 11502–11513. PMLR.
- Zwillinger, D., Moll, V., Gradshteyn, I., and Ryzhik, I., editors (2014). *Table of Integrals, Series, and Products*. Academic Press, Boston, eighth edition.

A Proofs

Proof of Proposition 1.1. The first implication follows directly from the derivation of the Laplace–Beltrami operator as a Stein operator of the uniform law. In fact, for any smooth function f , the relation $\mathbb{E}_{\mathcal{H}_0} [\Delta_{\mathcal{S}^{p-1}} f(\mathbf{X})] = 0$ holds. Choosing $f(\mathbf{x}) = e^{\lambda \mathbf{t}^\top \mathbf{x}}$ yields $\mathbb{E}[\Delta_{\mathcal{S}^{p-1}} e^{\lambda \mathbf{t}^\top \mathbf{X}}] = 0$ for all $\mathbf{t} \in \mathcal{S}^{p-1}$ and fixed $\lambda > 0$.

Further, for all fixed $\lambda > 0$, the function class $\{e^{\lambda \mathbf{t}^\top \mathbf{x}} : \mathbf{t} \in \mathcal{S}^{p-1}\}$ is indeed sufficient to characterize the distributions. Let q be the density of the random element \mathbf{X} on \mathcal{S}^{p-1} and $q \in L^2(\mathcal{S}^{p-1})$, and assume that $\mathbb{E}[\Delta_{\mathcal{S}^{p-1}} e^{\lambda \mathbf{t}^\top \mathbf{X}}] = 0$ for all $\mathbf{t} \in \mathcal{S}^{p-1}$. Then, with the harmonic expansion $q(\mathbf{x}) = \sum_{k=0}^{\infty} \sum_{r=1}^{d_{k,p}} \beta_{r,k} Y_{r,k}(\mathbf{x})$, $\mathbf{x} \in \mathcal{S}^{p-1}$, we find

$$\begin{aligned} \mathbb{E} \left[\Delta_{\mathcal{S}^{p-1}} e^{\lambda \mathbf{t}^\top \mathbf{X}} \right] &= \int_{\mathcal{S}^{p-1}} \sum_{k=0}^{\infty} (-k)(k+p-2) m_{k,p}(\lambda) C_k^{(p-2)/2}(\mathbf{t}^\top \mathbf{x}) q(\mathbf{x}) \, d\nu_{p-1}(\mathbf{x}) \\ &= \sum_{k=0}^{\infty} (-k)(k+p-2) m_{k,p}(\lambda) \sum_{r=1}^{d_{k,p}} \beta_{r,k} \int_{\mathcal{S}^{p-1}} C_k^{(p-2)/2}(\mathbf{t}^\top \mathbf{x}) Y_{r,k}(\mathbf{x}) \, d\nu_{p-1}(\mathbf{x}). \end{aligned}$$

By the Funk–Hecke formula (Dai and Xu, 2013, Theorem 1.2.9),

$$\int_{\mathcal{S}^{p-1}} C_k^{(p-2)/2}(\mathbf{t}^\top \mathbf{x}) Y_{r,k}(\mathbf{x}) \, d\nu_{p-1}(\mathbf{x}) = \frac{\omega_{p-2} h_{k,p}}{\omega_{p-1} C_k^{(p-2)/2}(1)} Y_{r,k}(\mathbf{t}) = \gamma_{k,p} Y_{r,k}(\mathbf{t}),$$

with $\gamma_{k,p} \neq 0$ for $k \geq 1$, hence

$$\mathbb{E} \left[\Delta_{\mathcal{S}^{p-1}} e^{\lambda \mathbf{t}^\top \mathbf{X}} \right] = \sum_{k=0}^{\infty} (-k)(k+p-2) m_{k,p}(\lambda) \gamma_{k,p} \sum_{r=1}^{d_{k,p}} \beta_{r,k} Y_{r,k}(\mathbf{t})$$

holds. Since this function is identically zero, orthogonality implies $\beta_{r,k} = 0$ for all $k \geq 1$, hence q is constant ν_{p-1} -almost everywhere. Since $M_{\mathbf{X}}(\mathbf{0}) = 1$, q is indeed normalized and a density, and thus $\mathbf{X} \sim \text{Unif}(\mathcal{S}^{p-1})$. \square

Proof of Lemma 2.1. To derive the closed-form formulas of the coefficients, we consider the cases $p > 2$ and $p = 2$ separately. First, for $p > 2$, we use the series expansion (4), the eigenfunction relation of the Gegenbauer polynomials, the uniform convergence of the series (see Remark 2.1), and the Funk–Hecke formula (7), to see

$$\begin{aligned} T_n(\lambda) &= n \int_{\mathcal{S}^{p-1}} \left| \frac{1}{n} \sum_{i=1}^n \Delta_{\mathcal{S}^{p-1}} e^{\lambda \mathbf{t}^\top \mathbf{X}_i} \right|^2 \, d\nu_{p-1}(\mathbf{t}) \\ &= \frac{1}{n} \sum_{i,j=1}^n \int_{\mathcal{S}^{p-1}} \left(\sum_{k=0}^{\infty} m_{k,p}(\lambda) (-k)(k+p-2) C_k^{(p-2)/2}(\mathbf{t}^\top \mathbf{X}_i) \right) \\ &\quad \times \left(\sum_{\ell=0}^{\infty} m_{\ell,p}(\lambda) (-\ell)(\ell+p-2) C_\ell^{(p-2)/2}(\mathbf{t}^\top \mathbf{X}_j) \right) \, d\nu_{p-1}(\mathbf{t}) \\ &= \frac{1}{n} \sum_{i,j=1}^n \sum_{k,\ell=1}^{\infty} m_{k,p}(\lambda) (-k)(k+p-2) m_{\ell,p}(\lambda) (-\ell)(\ell+p-2) \\ &\quad \times \int_{\mathcal{S}^{p-1}} C_k^{(p-2)/2}(\mathbf{t}^\top \mathbf{X}_i) C_\ell^{(p-2)/2}(\mathbf{t}^\top \mathbf{X}_j) \, d\nu_{p-1}(\mathbf{t}) \\ &= \frac{1}{n} \sum_{i,j=1}^n \sum_{k=1}^{\infty} (m_{k,p}(\lambda) k(k+p-2))^2 \frac{p-2}{2k+p-2} C_k^{(p-2)/2}(\mathbf{X}_i^\top \mathbf{X}_j). \end{aligned}$$

By plugging in expression (5), the resulting coefficients are

$$\begin{aligned}
c_{k,p}(\lambda) &= (m_{k,p}(\lambda)k(k+p-2))^2 \gamma_{k,p} \\
&= \left(\left(\frac{2}{\lambda} \right)^{(p-2)/2} \Gamma \left(\frac{p-2}{2} \right) \left(k + \frac{p-2}{2} \right) \mathcal{I}_{(p-2)/2+k}(\lambda) k(k+p-2) \right)^2 \frac{p-2}{2k+p-2} \\
&= 2^{p-3} \lambda^{2-p} (p-2) \left(k + \frac{p-2}{2} \right) \left(\Gamma \left(\frac{p-2}{2} \right) k(k+p-2) \mathcal{I}_{(p-2)/2+k}(\lambda) \right)^2.
\end{aligned}$$

For $p = 2$, we get, in analogy to the case $p > 2$,

$$\begin{aligned}
\Delta_{\mathcal{S}^{p-1}} e^{\lambda \mathbf{t}^\top \mathbf{x}} &= \Delta_{\mathcal{S}^{p-1}} \sum_{k=0}^{\infty} m_{k,2}(\lambda) C_k^0(\mathbf{t}^\top \mathbf{x}) \\
&= \sum_{k=0}^{\infty} m_{k,2}(\lambda) \Delta_{\mathcal{S}^{p-1}} C_k^0(\mathbf{t}^\top \mathbf{x}) = \sum_{k=0}^{\infty} m_{k,2}(\lambda) (-k^2) C_k^0(\mathbf{t}^\top \mathbf{x}).
\end{aligned}$$

Thus, we obtain with this expansion

$$\begin{aligned}
T_n(\lambda) &= n \int_{\mathcal{S}^1} \left| \frac{1}{n} \sum_{i=1}^n \Delta_{\mathcal{S}^1} e^{\lambda \mathbf{t}^\top \mathbf{X}_i} \right|^2 d\nu_1(\mathbf{t}) \\
&= \frac{1}{n} \sum_{i,j=1}^n \sum_{k,\ell=1}^{\infty} m_{k,2}(\lambda) (-k^2) m_{\ell,2}(\lambda) (-\ell^2) \int_{\mathcal{S}^1} C_k^0(\mathbf{t}^\top \mathbf{X}_i) C_\ell^0(\mathbf{t}^\top \mathbf{X}_j) d\nu_1(\mathbf{t}) \\
&= \frac{1}{n} \sum_{i,j=1}^n \sum_{k=1}^{\infty} (m_{k,2}(\lambda) k^2)^2 \frac{1 + 1_{\{k=0\}}}{2} C_k^0(\mathbf{X}_i^\top \mathbf{X}_j) = \frac{1}{n} \sum_{i,j=1}^n \sum_{k=1}^{\infty} (m_{k,2}(\lambda) k^2)^2 \gamma_{k,2} C_k^0(\mathbf{X}_i^\top \mathbf{X}_j).
\end{aligned}$$

Hence, we conclude

$$c_{k,2}(\lambda) = (m_{k,2}(\lambda) k^2)^2 \frac{1 + 1_{\{k=0\}}}{2} = \left(\frac{\mathcal{I}_k(\lambda)}{(1 + 1_{\{k=0\}})/2} k^2 \right)^2 \frac{1 + 1_{\{k=0\}}}{2} = (2 - 1_{\{k=0\}}) k^4 \mathcal{I}_k(\lambda)^2$$

in the two-dimensional case. Here, the case $k = 0$ can be discarded, since k is a factor of $c_{k,2}$.

The test statistic for general $p \geq 2$ can be expressed, combining both cases, as

$$T_n(\lambda) = \frac{1}{n} \sum_{i,j=1}^n \sum_{k=1}^{\infty} c_{k,p}(\lambda) C_k^{(p-2)/2}(\mathbf{X}_i^\top \mathbf{X}_j).$$

□

Proof of Theorem 3.1. This result follows from the central limit theorem in Hilbert spaces (Henze, 2024, Theorem 17.29), since for

$$\Psi(\mathbf{t}, \mathbf{x}) = \Delta_{\mathcal{S}^{p-1}} e^{\lambda \mathbf{t}^\top \mathbf{x}} = \sum_{k=0}^{\infty} m_{k,p}(\lambda) (-k)(k+p-2) C_k^{(p-2)/2}(\mathbf{t}^\top \mathbf{x}), \quad (21)$$

we have $W_n(\mathbf{t}) = n^{-1/2} \sum_{i=1}^n \Psi(\mathbf{t}, \mathbf{X}_i)$. Here, the summands are iid and centered elements in $L^2(\mathcal{S}^{p-1})$, i.e., $\mathbb{E}[\Psi(\cdot, \mathbf{X})] = 0$, since $\mathbb{E}[\Psi(\mathbf{t}, \mathbf{X})] = 0$ for all $\mathbf{t} \in \mathcal{S}^{p-1}$, and have finite second moment

$$\mathbb{E} \left[\|\Psi(\cdot, \mathbf{X})\|_{L^2(\mathcal{S}^{p-1})}^2 \right] = \sum_{k=0}^{\infty} (m_{k,p}(\lambda) (-k)(k+p-2))^2 \mathbb{E} \left[\int_{\mathcal{S}^{p-1}} \{C_k^{(p-2)/2}(\mathbf{t}^\top \mathbf{X})\}^2 d\nu_{p-1}(\mathbf{t}) \right] \quad (22)$$

$$= \sum_{k=1}^{\infty} c_{k,p}(\lambda) C_k^{(p-2)/2}(1) < \infty.$$

This allows direct application of Henze (2024, Theorem 17.29), implying $W_n \xrightarrow{d} \mathcal{W}$ for a centered Gaussian process \mathcal{W} with the covariance kernel

$$\begin{aligned} K(\mathbf{s}, \mathbf{t}) &= \mathbb{E} [\Psi(\mathbf{s}, \mathbf{X}) \Psi(\mathbf{t}, \mathbf{X})] \\ &= \mathbb{E} \left[\sum_{k=0}^{\infty} m_{k,p}(\lambda) (-k)(k+p-2) C_k^{(p-2)/2}(\mathbf{s}^\top \mathbf{X}) \sum_{\ell=0}^{\infty} m_{\ell,p}(\lambda) (-\ell)(\ell+p-2) C_\ell^{(p-2)/2}(\mathbf{t}^\top \mathbf{X}) \right] \\ &= \sum_{k,\ell=0}^{\infty} m_{k,p}(\lambda) (-k)(k+p-2) m_{\ell,p}(\lambda) (-\ell)(\ell+p-2) \mathbb{E} \left[C_k^{(p-2)/2}(\mathbf{s}^\top \mathbf{X}) C_\ell^{(p-2)/2}(\mathbf{t}^\top \mathbf{X}) \right] \\ &= \sum_{k=0}^{\infty} (m_{k,p}(\lambda) k(k+p-2))^2 \gamma_{k,p} C_k^{(p-2)/2}(\mathbf{s}^\top \mathbf{t}) = \sum_{k=0}^{\infty} c_{k,p}(\lambda) C_k^{(p-2)/2}(\mathbf{s}^\top \mathbf{t}). \end{aligned}$$

□

Proof of Theorem 3.2. We prove this result by applying the Karhunen–Loève expansion (Henze, 2024, Theorem 17.26) to the limiting Gaussian element \mathcal{W} from Theorem 3.1. To this end, we find the eigenvalues $\alpha_{m,k}$ of the covariance operator C defined by

$$Cf(\mathbf{x}) = \int_{\mathcal{S}^{p-1}} K(\mathbf{s}, \mathbf{x}) f(\mathbf{s}) d\nu_{p-1}(\mathbf{s}), \quad \mathbf{x} \in \mathcal{S}^{p-1}, \quad f \in L^2(\mathcal{S}^{p-1}).$$

This can be done for the basis of spherical harmonic functions $\{Y_{r,k} : r = 1, \dots, d_{k,p}\}$ of degree $k \in \mathbb{N}_0$, again by using uniform convergence and the Funk–Hecke formula (for $1 \leq r \leq d_{k,p}$):

$$\begin{aligned} CY_{r,k}(\mathbf{x}) &= \int_{\mathcal{S}^{p-1}} \sum_{m=0}^{\infty} c_{m,p}(\lambda) C_m^{(p-2)/2}(\mathbf{s}^\top \mathbf{x}) Y_{r,k}(\mathbf{s}) d\nu_{p-1}(\mathbf{s}) \\ &= \sum_{m=0}^{\infty} c_{m,p}(\lambda) \int_{\mathcal{S}^{p-1}} C_m^{(p-2)/2}(\mathbf{s}^\top \mathbf{x}) Y_{r,k}(\mathbf{s}) d\nu_{p-1}(\mathbf{s}) = \sum_{m=0}^{\infty} c_{m,p}(\lambda) \alpha_{m,k} Y_{r,k}(\mathbf{x}). \end{aligned}$$

Here, we write

$$\alpha_{m,k} = \frac{\omega_{p-2}}{\omega_{p-1} C_m^{(p-2)/2}(1)} \int_{-1}^1 C_k^{(p-2)/2}(t) C_m^{(p-2)/2}(t) (1-t^2)^{(p-3)/2} dt = 1_{\{m=k\}} \gamma_{k,p},$$

so the resulting eigenvalues take the form

$$CY_{r,k}(\mathbf{x}) = c_{k,p}(\lambda) \gamma_{k,p} Y_{r,k}(\mathbf{x}).$$

Note that, for any degree k , there are $d_{k,p}$ spherical harmonics, so together with Theorem 3.1 we obtain

$$T_n(\lambda) \xrightarrow{d} \|\mathcal{W}\|_{L^2(\mathcal{S}^{p-1})}^2,$$

for the centered Gaussian element \mathcal{W} .

Moreover, $\mathbb{E}[\langle \mathcal{W}, Y_{r,k} \rangle_{L^2(\mathcal{S}^{p-1})}^2] = c_{k,p}(\lambda) \gamma_{k,p}$, so $\langle \mathcal{W}, Y_{r,k} \rangle_{L^2(\mathcal{S}^{p-1})} \sim \mathcal{N}(0, c_{k,p}(\lambda) \gamma_{k,p})$, therefore,

$$\|\mathcal{W}\|_{L^2(\mathcal{S}^{p-1})}^2 = \sum_{k=1}^{\infty} \sum_{r=1}^{d_{k,p}} \langle \mathcal{W}, Y_{r,k} \rangle_{L^2(\mathcal{S}^{p-1})}^2 = \sum_{k=1}^{\infty} \sum_{r=1}^{d_{k,p}} c_{k,p}(\lambda) \gamma_{k,p} N_{k,r}^2,$$

where all $N_{k,r}$ are independent standard normally distributed random variables, so the stated result follows. \square

Proof of Lemma 3.1. Let $\mathbf{t} \in \mathbb{R}^p \setminus \{\mathbf{0}\}$ and write $\mathbf{u} := \mathbf{t}/\|\mathbf{t}\| \in \mathcal{S}^{p-1}$. Using the harmonic decomposition (10), its convergence in $L^2(\mathcal{S}^{p-1})$ and Funk–Hecke formula (7), we obtain

$$\begin{aligned}
M_{\mathbf{X}}(\lambda \mathbf{t}) &= \int_{\mathcal{S}^{p-1}} e^{\lambda \mathbf{t}^\top \mathbf{x}} q(\mathbf{x}) \, d\nu_{p-1}(\mathbf{x}) = \int_{\mathcal{S}^{p-1}} e^{\lambda \mathbf{t}^\top \mathbf{x}} \sum_{k=0}^{\infty} \sum_{r=1}^{d_{k,p}} \beta_{r,k} Y_{r,k}(\mathbf{x}) \, d\nu_{p-1}(\mathbf{x}) \\
&= \sum_{k=0}^{\infty} \sum_{r=1}^{d_{k,p}} \beta_{r,k} \int_{\mathcal{S}^{p-1}} e^{\lambda \mathbf{t}^\top \mathbf{x}} Y_{r,k}(\mathbf{x}) \, d\nu_{p-1}(\mathbf{x}) = \sum_{k=0}^{\infty} \sum_{r=1}^{d_{k,p}} \beta_{r,k} \int_{\mathcal{S}^{p-1}} e^{\lambda \|\mathbf{t}\| \mathbf{u}^\top \mathbf{x}} Y_{r,k}(\mathbf{x}) \, d\nu_{p-1}(\mathbf{x}) \\
&= \sum_{k=0}^{\infty} \sum_{r=1}^{d_{k,p}} \beta_{r,k} m_{k,p}(\lambda \|\mathbf{t}\|) \int_{\mathcal{S}^{p-1}} C_k^{(p-2)/2}(\mathbf{u}^\top \mathbf{x}) Y_{r,k}(\mathbf{x}) \, d\nu_{p-1}(\mathbf{x}) \\
&= \sum_{k=0}^{\infty} \sum_{r=1}^{d_{k,p}} \beta_{r,k} m_{k,p}(\lambda \|\mathbf{t}\|) \gamma_{k,p} Y_{r,k}(\mathbf{u})
\end{aligned}$$

in $L^2(\mathcal{S}^{p-1})$.

Fixing $\|\mathbf{t}\| = 1$, by restricting the function to the sphere, the only dependence of $M_{\mathbf{X}}$ on \mathbf{t} is in the spherical harmonic $Y_{r,k}$. Here, we use again the fact that the spherical harmonics form the eigenfunctions of the Laplace–Beltrami operator, together with Remark 2.1 to derive for $\mathbf{s} \in \mathcal{S}^{p-1}$

$$\begin{aligned}
z(\mathbf{s}) &= \Delta_{\mathcal{S}^{p-1}} M_{\mathbf{X}}(\lambda \mathbf{s}) = \int_{\mathcal{S}^{p-1}} \Delta_{\mathcal{S}^{p-1}, \mathbf{s}} e^{\lambda \mathbf{s}^\top \mathbf{x}} q(\mathbf{x}) \, d\nu_{p-1}(\mathbf{x}) \\
&= \int_{\mathcal{S}^{p-1}} \sum_{k=0}^{\infty} m_{k,p}(\lambda) \Delta_{\mathcal{S}^{p-1}, \mathbf{s}} C_k^{(p-2)/2}(\mathbf{s}^\top \mathbf{x}) \sum_{\ell=0}^{\infty} \sum_{r=1}^{d_{\ell,p}} \beta_{r,\ell} Y_{r,\ell}(\mathbf{x}) \, d\nu_{p-1}(\mathbf{x}) \\
&= \sum_{k=0}^{\infty} \sum_{\ell=0}^{\infty} \sum_{r=1}^{d_{k,p}} m_{k,p}(\lambda) (-k)(k+p-2) \beta_{r,\ell} \int_{\mathcal{S}^{p-1}} C_k^{(p-2)/2}(\mathbf{s}^\top \mathbf{x}) Y_{r,\ell}(\mathbf{x}) \, d\nu_{p-1}(\mathbf{x}) \\
&= \sum_{k=0}^{\infty} \sum_{r=1}^{d_{k,p}} \beta_{r,k} m_{k,p}(\lambda) \gamma_{k,p} (-k)(k+p-2) Y_{r,k}(\mathbf{s}).
\end{aligned}$$

Again, by using decomposition (10), we derive the equality in $L^2(\mathcal{S}^{p-1})$. \square

Proof of Theorem 3.3. For the process $W_n(\mathbf{t})$ use (21) to write $W_n(\mathbf{t}) = n^{-1/2} \sum_{i=1}^n \Psi(\mathbf{t}, \mathbf{X}_i)$. Since $\mathbb{E}[\|\Psi(\mathbf{t}, \mathbf{X})\|_{L^2(\mathcal{S}^{p-1})}^2] = \sum_{k=0}^{\infty} c_{k,p}(\lambda) C_k^{(p-2)/2}(1) < \infty$, see (22), by the strong law of large numbers in Hilbert spaces (Henze, 2024, Theorem 17.15) we obtain

$$\frac{T_n(\lambda)}{n} = \frac{\|W_n\|_{L^2(\mathcal{S}^{p-1})}^2}{n} = \left\| \frac{1}{n} \sum_{i=1}^n \Psi(\cdot, \mathbf{X}_i) \right\|_{L^2(\mathcal{S}^{p-1})}^2 \xrightarrow{a.s.} \|z\|_{L^2(\mathcal{S}^{p-1})}^2.$$

In Lemma 3.1, we represent z in terms of spherical harmonics in $L^2(\mathcal{S}^{p-1})$. In particular

$$\langle z, Y_{r,k} \rangle_{L^2(\mathcal{S}^{p-1})} = (\beta_{r,k} \gamma_{k,p} m_{k,p}(\lambda) (-k)(k+p-2)),$$

and Parseval's Identity yields

$$\tau = \|z\|_{L^2(\mathcal{S}^{p-1})}^2 = \sum_{k=0}^{\infty} \sum_{r=1}^{d_{k,p}} \langle z, Y_{r,k} \rangle_{L^2(\mathcal{S}^{p-1})}^2 = \sum_{k=0}^{\infty} \sum_{r=1}^{d_{k,p}} (\beta_{r,k} \gamma_{k,p} m_{k,p}(\lambda) (-k)(k+p-2))^2, \quad (23)$$

since the harmonics form an orthonormal basis of $L^2(\mathcal{S}^{p-1})$. \square

Proof of Theorem 3.4. We write the centered process by definition as

$$(W_n - \sqrt{n}z) = \frac{1}{\sqrt{n}} \sum_{i=1}^n (\Delta_{\mathcal{S}^{p-1}} e^{\lambda \mathbf{t}^\top \mathbf{X}_i} - \Delta_{\mathcal{S}^{p-1}} M_{\mathbf{X}}(\lambda \mathbf{t})),$$

where the terms $\Delta_{\mathcal{S}^{p-1}} e^{\lambda \mathbf{t}^\top \mathbf{X}_i} - \Delta_{\mathcal{S}^{p-1}} M_{\mathbf{X}}(\lambda \mathbf{t}) \in L^2(\mathcal{S}^{p-1})$ are iid, square-integrable random functions. Furthermore, $\mathbb{E}[\Delta_{\mathcal{S}^{p-1}} e^{\lambda \mathbf{t}^\top \mathbf{X}_i} - \Delta_{\mathcal{S}^{p-1}} M_{\mathbf{X}}(\lambda \mathbf{t})] = 0$ and with (22),

$$\begin{aligned} & \mathbb{E} \left[\left\| \Delta_{\mathcal{S}^{p-1}} e^{\lambda \mathbf{t}^\top \mathbf{X}_i} - \Delta_{\mathcal{S}^{p-1}} M_{\mathbf{X}}(\lambda \mathbf{t}) \right\|_{L^2(\mathcal{S}^{p-1})}^2 \right] \\ &= \mathbb{E} \left[\left\| \Delta_{\mathcal{S}^{p-1}} e^{\lambda \mathbf{t}^\top \mathbf{X}_i} \right\|_{L^2(\mathcal{S}^{p-1})}^2 \right] - \left\| \Delta_{\mathcal{S}^{p-1}} M_{\mathbf{X}}(\lambda \mathbf{t}) \right\|_{L^2(\mathcal{S}^{p-1})}^2 < \infty, \end{aligned}$$

so direct application of the central limit theorem in Hilbert spaces (Henze, 2024, Theorem 17.29) yields a centered Gaussian limit process, with covariance kernel

$$\begin{aligned} K'(\mathbf{s}, \mathbf{t}) &= \mathbb{E} \left[\left(\Delta_{\mathcal{S}^{p-1}} e^{\lambda \mathbf{s}^\top \mathbf{X}} - \Delta_{\mathcal{S}^{p-1}} M_{\mathbf{X}}(\lambda \mathbf{s}) \right) \left(\Delta_{\mathcal{S}^{p-1}} e^{\lambda \mathbf{t}^\top \mathbf{X}} - \Delta_{\mathcal{S}^{p-1}} M_{\mathbf{X}}(\lambda \mathbf{t}) \right) \right] \\ &= \mathbb{E} \left[\Delta_{\mathcal{S}^{p-1}} e^{\lambda \mathbf{s}^\top \mathbf{X}} \Delta_{\mathcal{S}^{p-1}} e^{\lambda \mathbf{t}^\top \mathbf{X}} \right] - \Delta_{\mathcal{S}^{p-1}} M_{\mathbf{X}}(\lambda \mathbf{s}) \Delta_{\mathcal{S}^{p-1}} M_{\mathbf{X}}(\lambda \mathbf{t}). \end{aligned}$$

Plugging in the definition and exploiting the symmetry of the operator, we find

$$\begin{aligned} \Delta_{\mathcal{S}^{p-1}} e^{\lambda \mathbf{s}^\top \mathbf{x}} \Delta_{\mathcal{S}^{p-1}} e^{\lambda \mathbf{t}^\top \mathbf{x}} &= \left(\lambda(1-p) \lambda \mathbf{x}^\top \nabla e^{\lambda \mathbf{s}^\top \mathbf{x}} - \lambda^2 \mathbf{x}^\top \nabla^2 e^{\lambda \mathbf{s}^\top \mathbf{x}} \mathbf{x} + \lambda^2 \Delta e^{\lambda \mathbf{s}^\top \mathbf{x}} \right) \\ &\quad \times \left(\lambda(1-p) \mathbf{x}^\top \nabla e^{\lambda \mathbf{t}^\top \mathbf{x}} - \lambda^2 \mathbf{x}^\top \nabla^2 e^{\lambda \mathbf{t}^\top \mathbf{x}} \mathbf{x} + \lambda^2 \Delta e^{\lambda \mathbf{t}^\top \mathbf{x}} \right) \\ &= \Delta_{\mathcal{S}^{p-1}, \mathbf{s}} \Delta_{\mathcal{S}^{p-1}, \mathbf{t}} e^{\lambda(\mathbf{s}+\mathbf{t})^\top \mathbf{x}}, \end{aligned}$$

which implies

$$\mathbb{E} \left[\Delta_{\mathcal{S}^{p-1}} e^{\lambda \mathbf{s}^\top \mathbf{X}} \Delta_{\mathcal{S}^{p-1}} e^{\lambda \mathbf{t}^\top \mathbf{X}} \right] = \Delta_{\mathcal{S}^{p-1}, \mathbf{s}} \Delta_{\mathcal{S}^{p-1}, \mathbf{t}} M_{\mathbf{X}}(\lambda(\mathbf{s} + \mathbf{t})).$$

For the second representation of this term, we expand the initial representation in Gegenbauer polynomials

$$\begin{aligned} \mathbb{E} \left[\Delta_{\mathcal{S}^{p-1}} e^{\lambda \mathbf{s}^\top \mathbf{X}} \Delta_{\mathcal{S}^{p-1}} e^{\lambda \mathbf{t}^\top \mathbf{X}} \right] &= \int_{\mathcal{S}^{p-1}} \sum_{k_1=0}^{\infty} (m_{k_1, p}(\lambda) (-k_1)(k_1 + p - 2)) C_{k_1}^{(p-2)/2}(\mathbf{s}^\top \mathbf{x}) \\ &\quad \times \sum_{k_2=0}^{\infty} (m_{k_2, p}(\lambda) (-k_2)(k_2 + p - 2)) C_{k_2}^{(p-2)/2}(\mathbf{t}^\top \mathbf{x}) q(\mathbf{x}) d\nu_{p-1}(\mathbf{x}) \\ &= \sum_{k_1=0}^{\infty} \sum_{k_2=0}^{\infty} (m_{k_1, p}(\lambda) (-k_1)(k_1 + p - 2)) (m_{k_2, p}(\lambda) (-k_2)(k_2 + p - 2)) \\ &\quad \times \int_{\mathcal{S}^{p-1}} C_{k_1}^{(p-2)/2}(\mathbf{s}^\top \mathbf{x}) C_{k_2}^{(p-2)/2}(\mathbf{t}^\top \mathbf{x}) q(\mathbf{x}) d\nu_{p-1}(\mathbf{x}) \\ &= \sum_{k_1=0}^{\infty} \sum_{k_2=0}^{\infty} (m_{k_1, p}(\lambda) (-k_1)(k_1 + p - 2)) (m_{k_2, p}(\lambda) (-k_2)(k_2 + p - 2)) \\ &\quad \times \mathbb{E} \left[C_{k_1}^{(p-2)/2}(\mathbf{s}^\top \mathbf{X}) C_{k_2}^{(p-2)/2}(\mathbf{t}^\top \mathbf{X}) \right]. \end{aligned}$$

Defining the shorthand notation $\xi_{k_1, k_2}(\mathbf{s}, \mathbf{t}) = \mathbb{E} \left[C_{k_1}^{(p-2)/2}(\mathbf{s}^\top \mathbf{X}) C_{k_2}^{(p-2)/2}(\mathbf{t}^\top \mathbf{X}) \right]$ yields the desired representation. \square

Proof of Theorem 3.5. We proceed as in Baringhaus et al. (2017) to obtain the distribution of the centered test statistic,

$$\begin{aligned}\sqrt{n} \left(\frac{T_n(\lambda)}{n} - \tau \right) &= \sqrt{n} \left(\left\| \frac{W_n}{\sqrt{n}} \right\|_{L^2(\mathcal{S}^{p-1})}^2 - \|z\|_{L^2(\mathcal{S}^{p-1})}^2 \right) = \sqrt{n} \left\langle \frac{W_n}{\sqrt{n}} - z, \frac{W_n}{\sqrt{n}} + z \right\rangle_{L^2(\mathcal{S}^{p-1})} \\ &= \sqrt{n} \left\langle \frac{W_n}{\sqrt{n}} - z, 2z + \frac{W_n}{\sqrt{n}} - z \right\rangle_{L^2(\mathcal{S}^{p-1})} \\ &= 2 \left\langle \sqrt{n} \left(\frac{W_n}{\sqrt{n}} - z \right), z \right\rangle_{L^2(\mathcal{S}^{p-1})} + \frac{1}{\sqrt{n}} \left\| \sqrt{n} \left(\frac{W_n}{\sqrt{n}} - z \right) \right\|_{L^2(\mathcal{S}^{p-1})}^2.\end{aligned}$$

In Theorem 3.4, we saw the convergence of $\sqrt{n}(W_n/\sqrt{n} - z)$ to a centered Gaussian element in $L^2(\mathcal{S}^{p-1})$. By Slutsky's lemma and the continuous mapping theorem, $\sqrt{n}(T_n(\lambda)/n - \tau) \xrightarrow{d} 2 \langle \mathcal{W}', z \rangle$. Here, $2 \langle \mathcal{W}', z \rangle$ is centered normal distributed with variance $\mathbb{E}[4 \langle \mathcal{W}', z \rangle^2]$. With Fubini's theorem and applying K' from Theorem 3.4, we derive

$$\begin{aligned}\sigma^2 &= 4 \int_{\mathcal{S}^{p-1}} \int_{\mathcal{S}^{p-1}} \mathbb{E} [\mathcal{W}'(\mathbf{s}) \mathcal{W}'(\mathbf{t})] z(\mathbf{s}) z(\mathbf{t}) d\nu_{p-1}(\mathbf{s}) d\nu_{p-1}(\mathbf{t}) \\ &= 4 \int_{\mathcal{S}^{p-1}} \int_{\mathcal{S}^{p-1}} K'(\mathbf{s}, \mathbf{t}) z(\mathbf{s}) z(\mathbf{t}) d\nu_{p-1}(\mathbf{s}) d\nu_{p-1}(\mathbf{t}) \\ &= 4 \int_{\mathcal{S}^{p-1}} \int_{\mathcal{S}^{p-1}} \left(\sum_{k_1=0}^{\infty} \sum_{k_2=0}^{\infty} (m_{k_1,p}(\lambda)(-k_1)(k_1+p-2)) (m_{k_2,p}(\lambda)(-k_2)(k_2+p-2)) \xi_{k_1,k_2}(\mathbf{s}, \mathbf{t}) \right) \\ &\quad \times z(\mathbf{s}) z(\mathbf{t}) d\nu_{p-1}(\mathbf{s}) d\nu_{p-1}(\mathbf{t}) - 4 \int_{\mathcal{S}^{p-1}} \int_{\mathcal{S}^{p-1}} z(\mathbf{s}) z(\mathbf{t}) z(\mathbf{s}) z(\mathbf{t}) d\nu_{p-1}(\mathbf{s}) d\nu_{p-1}(\mathbf{t}).\end{aligned}$$

We start by considering the first term in σ^2 and simplify the double integral by applying Fubini's theorem:

$$\begin{aligned}\int_{\mathcal{S}^{p-1}} \int_{\mathcal{S}^{p-1}} \xi_{k_1,k_2}(\mathbf{s}, \mathbf{t}) z(\mathbf{s}) z(\mathbf{t}) d\nu_{p-1}(\mathbf{s}) d\nu_{p-1}(\mathbf{t}) \\ = \mathbb{E} \left[\int_{\mathcal{S}^{p-1}} C_{k_1}^{(p-2)/2}(\mathbf{s}^\top \mathbf{X}) z(\mathbf{s}) d\nu_{p-1}(\mathbf{s}) \int_{\mathcal{S}^{p-1}} C_{k_2}^{(p-2)/2}(\mathbf{t}^\top \mathbf{X}) z(\mathbf{t}) d\nu_{p-1}(\mathbf{t}) \right].\end{aligned}$$

Let \mathbf{Y} denote an independent copy of \mathbf{X} , appearing in the definition of z , to separate the expectations. By applying Lemma 3.1 and changing the order of integration, we derive

$$\begin{aligned}\int_{\mathcal{S}^{p-1}} C_{k_2}^{(p-2)/2}(\mathbf{t}^\top \mathbf{x}) z(\mathbf{t}) d\nu_{p-1}(\mathbf{t}) \\ = \mathbb{E}_{\mathbf{Y}} \left[\int_{\mathcal{S}^{p-1}} C_{k_2}^{(p-2)/2}(\mathbf{t}^\top \mathbf{x}) \Delta_{\mathcal{S}^{p-1}} e^{\lambda \mathbf{t}^\top \mathbf{Y}} d\nu_{p-1}(\mathbf{t}) \right] \\ = \mathbb{E}_{\mathbf{Y}} \left[\int_{\mathcal{S}^{p-1}} C_{k_2}^{(p-2)/2}(\mathbf{t}^\top \mathbf{x}) \sum_{k=0}^{\infty} (m_{k,p}(\lambda)(-k)(k+p-2)) C_k^{(p-2)/2}(\mathbf{t}^\top \mathbf{Y}) d\nu_{p-1}(\mathbf{t}) \right] \\ = (m_{k_2,p}(\lambda)(-k_2)(k_2+p-2)) \mathbb{E}_{\mathbf{Y}} \left[\gamma_{k_2,p} C_{k_2}^{(p-2)/2}(\mathbf{Y}^\top \mathbf{x}) \right] \\ = (m_{k_2,p}(\lambda)(-k_2)(k_2+p-2)) \gamma_{k_2,p} \int_{\mathcal{S}^{p-1}} C_{k_2}^{(p-2)/2}(\mathbf{y}^\top \mathbf{x}) q(\mathbf{y}) d\nu_{p-1}(\mathbf{y}).\end{aligned}$$

We get by the addition formula of spherical harmonics, see Equation (1.2.8) in Dai and Xu (2013), and the definition of the spherical harmonic expansion coefficients in (11), that

$$\int_{\mathcal{S}^{p-1}} C_k^{(p-2)/2}(\mathbf{y}^\top \mathbf{x}) q(\mathbf{y}) d\nu_{p-1}(\mathbf{y}) = \int_{\mathcal{S}^{p-1}} \gamma_{k,p} \sum_{r=1}^{d_{k,p}} Y_{r,k}(\mathbf{y}) Y_{r,k}(\mathbf{x}) q(\mathbf{y}) d\nu_{p-1}(\mathbf{y})$$

$$= \gamma_{k,p} \sum_{r=1}^{d_{k,p}} Y_{r,k}(\mathbf{x}) \int_{\mathcal{S}^{p-1}} Y_{r,k}(\mathbf{y}) q(\mathbf{y}) d\nu_{p-1}(\mathbf{y}) = \gamma_{k,p} \sum_{r=1}^{d_{k,p}} Y_{r,k}(\mathbf{x}) \beta_{r,k}.$$

So, combining these results, we obtain

$$\begin{aligned} & \int_{\mathcal{S}^{p-1}} \int_{\mathcal{S}^{p-1}} \xi_{k_1, k_2}(\mathbf{s}, \mathbf{t}) z(\mathbf{s}) z(\mathbf{t}) d\nu_{p-1}(\mathbf{s}) d\nu_{p-1}(\mathbf{t}) \\ &= \mathbb{E} \left[(m_{k_1, p}(\lambda)(-k_1)(k_1 + p - 2)) \gamma_{k_1, p}^2 \sum_{r_1=1}^{d_{k_1, p}} Y_{r_1, k_1}(\mathbf{X}) \beta_{r_1, k_1} \right. \\ & \quad \left. \times (m_{k_2, p}(\lambda)(-k_2)(k_2 + p - 2)) \gamma_{k_2, p}^2 \sum_{r_2=1}^{d_{k_2, p}} Y_{r_2, k_2}(\mathbf{X}) \beta_{r_2, k_2} \right] \\ &= \sum_{r_1=1}^{d_{k_1, p}} \sum_{r_2=1}^{d_{k_2, p}} \beta_{r_1, k_1} (m_{k_1, p}(\lambda)(-k_1)(k_1 + p - 2)) \gamma_{k_1, p}^2 \\ & \quad \times \beta_{r_2, k_2} (m_{k_2, p}(\lambda)(-k_2)(k_2 + p - 2)) \gamma_{k_2, p}^2 \mathbb{E} [Y_{r_1, k_1}(\mathbf{X}) Y_{r_2, k_2}(\mathbf{X})]. \end{aligned}$$

Taking the sum over all k_1, k_2 , the first term leads to

$$\begin{aligned} & \sum_{k_1=0}^{\infty} \sum_{k_2=0}^{\infty} \sum_{r_1=1}^{d_{k_1, p}} \sum_{r_2=1}^{d_{k_2, p}} (\gamma_{k_1, p} m_{k_1, p}(\lambda)(-k_1)(k_1 + p - 2))^2 (\gamma_{k_2, p} m_{k_2, p}(\lambda)(-k_2)(k_2 + p - 2))^2 \\ & \quad \times \beta_{r_1, k_1} \beta_{r_2, k_2} \mathbb{E} [Y_{r_1, k_1}(\mathbf{X}) Y_{r_2, k_2}(\mathbf{X})] \\ &= \sum_{k_1=0}^{\infty} \sum_{k_2=0}^{\infty} \sum_{r_1=1}^{d_{k_1, p}} \sum_{r_2=1}^{d_{k_2, p}} \gamma_{k_1, p}^2 c_{k_1, p} \gamma_{k_2, p}^2 c_{k_2, p} \beta_{r_1, k_1} \beta_{r_2, k_2} \mathbb{E} [Y_{r_1, k_1}(\mathbf{X}) Y_{r_2, k_2}(\mathbf{X})]. \end{aligned}$$

In the case of rotationally symmetric alternatives, we use the linearization formula DLMF (2020, Equation 18.18.22) to get the expression in Remark 3.7, since

$$\begin{aligned} \mathbb{E} [C_{k_1}(\boldsymbol{\mu}^\top \mathbf{X}) C_{k_2}(\boldsymbol{\mu}^\top \mathbf{X})] &= \sum_{k_3=0}^{\infty} \beta_{k_3} \int_{\mathcal{S}^{p-1}} \sum_{\ell=0}^{\min(k_1, k_2)} L_{k_1, k_2}^{(p)}(\ell) C_{k_1+k_2-2\ell}^{(p-2)/2}(\boldsymbol{\mu}^\top \mathbf{x}) C_{k_3}^{(p-2)/2}(\boldsymbol{\mu}^\top \mathbf{x}) d\nu_{p-1}(\mathbf{x}) \\ &= \sum_{k_3=0}^{\infty} \beta_{k_3} \sum_{\ell=0}^{\min(k_1, k_2)} L_{k_1, k_2}^{(p)}(\ell) \int_{\mathcal{S}^{p-1}} C_{k_1+k_2-2\ell}^{(p-2)/2}(\boldsymbol{\mu}^\top \mathbf{x}) C_{k_3}^{(p-2)/2}(\boldsymbol{\mu}^\top \mathbf{x}) d\nu_{p-1}(\mathbf{x}) \\ &= \sum_{\ell=0}^{\min(k_1, k_2)} \beta_{k_1+k_2-2\ell} L_{k_1, k_2}^{(p)}(\ell) \gamma_{k_1, p+k_2-2\ell} C_{k_1+k_2-2\ell}^{(p-2)/2}(1). \end{aligned}$$

For the second term in σ^2 , we exploit orthogonality of the spherical harmonics via Parseval's identity, which yields the representation in (23). Hence,

$$\int_{\mathcal{S}^{p-1}} \int_{\mathcal{S}^{p-1}} z(\mathbf{s}) z(\mathbf{t}) z(\mathbf{s}) z(\mathbf{t}) d\nu_{p-1}(\mathbf{s}) d\nu_{p-1}(\mathbf{t}) = \|z\|_{L^2(\mathcal{S}^{p-1})}^4 = \left(\sum_{k=0}^{\infty} \sum_{r=1}^{d_{k,p}} \beta_{r,k}^2 \gamma_{k,p}^2 c_{k,p}(\lambda) \right)^2,$$

which completes the derivation of the result. \square

Remark A.1. For the product of two Gegenbauer or Chebychev polynomials, evaluated at the same argument $y \in [-1, 1]$, we get

$$C_{k_1}^{(p-2)/2}(\mathbf{s}^\top \mathbf{x}) C_{k_2}^{(p-2)/2}(\mathbf{s}^\top \mathbf{x}) = \sum_{\ell=0}^{\min(k_1, k_2)} L_{k_1, k_2}^{(p)}(\ell) C_{k_1+k_2-2\ell}^{(p-2)/2}(\mathbf{s}^\top \mathbf{x}) \quad \text{for all } \mathbf{s}, \mathbf{x} \in \mathcal{S}^{p-1}, \quad (24)$$

where for $p \geq 3$ we apply the linearization formula (DLMF, 2020, 18.18.22) with

$$L_{k_1, k_2}^{(p)}(\ell) = \frac{(k_1 + k_2 + (p-2)/2 - 2\ell)(k_1 + k_2 - 2\ell)!}{(k_1 + k_2 + (p-2)/2 - \ell)\ell!(k_1 - \ell)!(k_2 - \ell)!} \\ \times \frac{((p-2)/2)_\ell ((p-2)/2)_{k_1 - \ell} ((p-2)/2)_{k_2 - \ell} ((p-2))_{k_1 + k_2 - \ell}}{((p-2)/2)_{k_1 + k_2 - \ell} ((p-2))_{k_1 + k_2 - 2\ell}}$$

and for $p = 2$ (DLMF, 2020, 18.18.21)

$$L_{k_1, k_2}^{(2)}(\ell) = \frac{1}{2}(1_{\{\ell=0\}} + 1_{\{\ell=\min(k_1, k_2)\}}).$$

Proof of Proposition 4.1. We first consider the case $\lambda \rightarrow \infty$. Solving the integration in (3) directly yields the expression in terms of the coefficient $m_{0,p}(\lambda \|\mathbf{X}_i + \mathbf{X}_j\|)$ from (5)

$$T_n(\lambda) = \frac{1}{n} \left\| \sum_{i=1}^n \Delta_{S^{p-1}} e^{\lambda \mathbf{t}^\top \mathbf{X}_i} \right\|_{L^2(S^{p-1})}^2 = \frac{1}{n} \sum_{i,j=1}^n \Delta_{S^{p-1}, \mathbf{X}_i} \Delta_{S^{p-1}, \mathbf{X}_j} \int_{S^{p-1}} e^{\lambda \mathbf{t}^\top (\mathbf{X}_i + \mathbf{X}_j)} d\nu_{p-1}(\mathbf{t}) \\ = \frac{1}{n} \sum_{i,j=1}^n \Delta_{S^{p-1}, \mathbf{X}_i} \Delta_{S^{p-1}, \mathbf{X}_j} m_{0,p}(\lambda \|\mathbf{X}_i + \mathbf{X}_j\|).$$

Here, we use the zonal structure resulting in $\Delta_{S^{p-1}, \mathbf{t}} e^{\lambda \mathbf{t}^\top \mathbf{X}_i} = \Delta_{S^{p-1}, \mathbf{X}_i} e^{\lambda \mathbf{t}^\top \mathbf{X}_i}$. Although summands are not explicitly written, this expression helps analyze the behavior of the test in the limit case $\lambda \rightarrow \infty$. For large λ , we use the Bessel function approximation $\mathcal{I}_k(a) \approx e^a / \sqrt{2\pi a}$ as $a \rightarrow \infty$ from DLMF (2020, 10.30.4) to get for $p \geq 3$ that

$$\Delta_{S^{p-1}, \mathbf{X}_i} \Delta_{S^{p-1}, \mathbf{X}_j} m_{0,p}(\lambda \|\mathbf{X}_i + \mathbf{X}_j\|) \\ = \Delta_{S^{p-1}, \mathbf{X}_i} \Delta_{S^{p-1}, \mathbf{X}_j} \left(\frac{2}{\lambda \|\mathbf{X}_i + \mathbf{X}_j\|} \right)^{(p-2)/2} \Gamma\left(\frac{p-2}{2}\right) \left(\frac{p-2}{2}\right) \mathcal{I}_{(p-2)/2}(\lambda \|\mathbf{X}_i + \mathbf{X}_j\|) \\ \approx p_\lambda(\|\mathbf{X}_i + \mathbf{X}_j\|) e^{\lambda \|\mathbf{X}_i + \mathbf{X}_j\|},$$

where for each fixed $u > 0$ there exist $C(u) > 0$ and an integer $m = m(p)$ such that $|p_\lambda(u)| \leq C(u)\lambda^m$ for all sufficiently large λ . In the case $p = 2$, the expression simplifies to

$$\Delta_{S^1}^{(\mathbf{X}_i)} \Delta_{S^1}^{(\mathbf{X}_j)} m_{0,2}(\lambda \|\mathbf{X}_i + \mathbf{X}_j\|) = \Delta_{S^1}^{(\mathbf{X}_i)} \Delta_{S^1}^{(\mathbf{X}_j)} \mathcal{I}_0(\lambda \|\mathbf{X}_i + \mathbf{X}_j\|) \approx p_\lambda(\|\mathbf{X}_i + \mathbf{X}_j\|) e^{\lambda \|\mathbf{X}_i + \mathbf{X}_j\|}.$$

Since $\mathcal{O}_{\mathbb{P}}(\log(p_\lambda)/\lambda)$ is dominated by $o_{\mathbb{P}}(1)$, for $\lambda \rightarrow \infty$, the U -statistic $T_n(\lambda) - D_n(\lambda)$ can be transformed to

$$\frac{1}{\lambda} \log(T_n(\lambda) - D_n(\lambda)) = \frac{1}{\lambda} \log \left(2 \sum_{i < j} \exp(\log(p_\lambda(\|\mathbf{X}_i + \mathbf{X}_j\|)) + \lambda \|\mathbf{X}_i + \mathbf{X}_j\|) \right) \\ = \frac{1}{\lambda} \log \left(\sum_{i < j} \exp \left(\lambda \left(\frac{\log(p_\lambda(\|\mathbf{X}_i + \mathbf{X}_j\|))}{\lambda} + \|\mathbf{X}_i + \mathbf{X}_j\| \right) \right) \right) + \frac{\log 2}{\lambda} \\ \rightarrow \max_{i < j} \|\mathbf{X}_i + \mathbf{X}_j\| + o_{\mathbb{P}}(1) \text{ for } \lambda \rightarrow \infty.$$

In the last step, we use the convergence of the LogSumExp to the maximum,

$$\lim_{a \rightarrow \infty} \frac{1}{a} \log \left(\sum_{i=1}^n \exp(ax_i) \right) = \max_{1 \leq i \leq n} x_i.$$

Due to the monotone nature of the transformations $t \mapsto 1/\lambda(t - D_n(\lambda))$ and $t \mapsto \sqrt{2 + 2t}$ and the convergence against the expression $\max_{i < j} \mathbf{X}_i^\top \mathbf{X}_j$ of the transformed test statistic, we conclude the equivalence of test decisions with the test of Cai et al. (2013).

In the case $\lambda \rightarrow 0$, by $\mathcal{I}_k(a) \approx (a/2)^k/\Gamma(k+1)$ for $a \rightarrow 0$ in DLMF (2020, 10.30.1) and the harmonic decomposition (9) for $p \geq 2$, we rescale the coefficients $c_{k,p}(\lambda)$ to see there exist constants $C_{k,p}, C_{k,p}^* > 0$ depending only on $p \geq 2, k \geq 1$ so that

$$\frac{c_{k,p}(\lambda)}{\lambda^2} = C_{k,p} \lambda^{-p} \mathcal{I}_{(p-2)/2+k}(\lambda)^2 \approx C_{k,p}^* \lambda^{-p+p-2+2k}, \quad \lambda \rightarrow 0.$$

Now, clearly

$$\lim_{\lambda \rightarrow 0} C_{k,p}^* \lambda^{-2+2k} = C_{k,p}^* 1_{\{k=1\}},$$

implies that the limit is equivalent to the Rayleigh (1919) test, since

$$\lim_{\lambda \rightarrow 0} \frac{T_n(\lambda)}{\lambda^2} = \frac{1}{n} \sum_{i,j=1}^n C_{1,p}^* C_1^{(p-2)/2} (\mathbf{X}_i^\top \mathbf{X}_j) \propto \frac{1}{n} \sum_{i,j=1}^n \mathbf{X}_i^\top \mathbf{X}_j.$$

□